Received: 21 November 2021 | Revised: 7 January 2022 | Accepted: 15 January 2022

DOI: 10.1002/jmor.21451

RESEARCH ARTICLE

Journal of morphology WILEY

The epithelial layers of the body wall in hornerid bryozoans (Stenolaemata: Cyclostomatida)

Yuta Tamberg | Peter B. Batson | Abigail M. Smith

Department of Marine Science, University of Otago, Dunedin, New Zealand

Correspondence
Yuta Tamberg, Department of Marine Science, University of Otago, PO Box 56, Dunedin, New Zealand.
Email: yutamberg@gmail.com

Abstract

Bryozoans are small colonial coelomates. They can be conceptualised as "origami-like" animals, composed of three complexly folded epithelial layers: epidermis of the zooidal/colonial body wall, gut epithelium and coelothelium. We investigated the general microanatomy and ultrastructure of the hornerid (Cyclostomatatida) body wall and polypide in four taxa, including three species of *Hornera* and one species belonging to an undescribed genus. We describe epithelia and their associated structures (e.g., ECM, cuticle) across all portions of the hornerid body wall, including the terminal membrane, vestibular wall, atrial sphincter, membranous sac and polypide–skeletal attachments. The classic coelomate body wall composition (epidermis–ECM–coelothelium) is only present in an unmodified form in the tentacle sheath. Deeper within a zooid it is retained exclusively in the attachment zones of the membranous sac: [skeleton]–tendon cell–ECM–coelothelium. A typical invertebrate pattern of epithelial organisation is a single, continuous sheet of polarised cells, connected by belt desmosomes and septate junctions, and resting on a collagenous extracellular matrix. Although previous studies demonstrated that polypide-specific epithelia of Horneridae follow this model, here we show that the body wall may show significant deviations. Cell layers can lose the basement membrane and/or continuity of cell cover and cell contacts. Moreover, in portions of the body wall, the cell layer appears to be missing altogether; the zooidal orifice is covered by a thin naked cuticle largely devoid of underlying cells. Since epithelium is a two-way barrier against entry and loss of materials, it is unclear how hornerids avoid substance loss, while maintaining intracolonial metabolite transport with imperfect, sometimes incomplete, cell layers along large portions of their outer body surface.

KEYWORDS
atrial sphincter, coelothelium, membranous sac

1 | INTRODUCTION

Bryozoans are small, colonial invertebrates living in marine and freshwater benthic environments. The phylum includes three classes: Phylactolaemata, Gymnolaemata and Stenolaemata. The Cyclostomatida is the only living order of the exclusively marine stenolaemates. Bryozoan colonies are made of individual asexually budded modules, called zooids, which are commonly polymorphic, as well as multizooidal/

This is an open access article under the terms of the Creative Commons Attribution-NonCommercial License, which permits use, distribution and reproduction in any medium, provided the original work is properly cited and is not used for commercial purposes.
© 2022 The Authors. *Journal of Morphology* published by Wiley Periodicals LLC.

extrazooidal elements. The feeding autozooids comprise an outer skeletal wall (ectocyst), the living layer/layers of tissues underlying the skeleton (endocyst), and the polypide—the soft-body part of the zooid which includes all its organs (Figure 1). Bryozoans are coelomic animals with a tripartite body wall, comprising epidermis, extracellular matrix (ECM) and the coelomic lining. In terms of epithelial tissue, bryozoans can be conceptualised as "origami-like" creatures, composed of nested and intricately folded layers. These layers include only three components: the epidermis of the body wall (including endocyst, and outer colonial walls in free-walled taxa), gut epithelia and coelothelia. Epithelial layers, regardless of their specialisation, form one of the four fundamental tissue types (Jonusaite et al., 2016) and are characterised by three key traits (Figure 2): cohesion through cell contacts, shared apical-basal cell polarisation, and basal ECM (reviewed e.g., by Tyler, 2003).

Although existing data is sparse, it appears that ectocyst (either mineralised or not) affects underlying local body wall composition in Gymnolaemata and Cyclostomatida, but not in Phylactolaemata (examples below). In all bryozoans a 'typical' coelomate body wall with epidermis, ECM, coelothelium and cell contacts is always present in the areas unsupported by skeleton, that is, tentacles and tentacle sheath, but the composition of the endocyst varies.

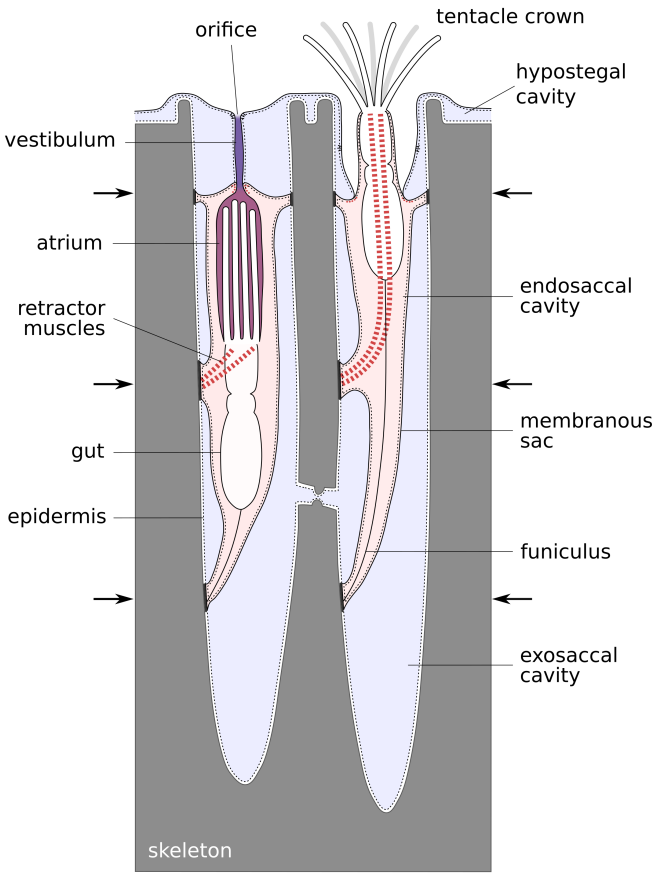

FIGURE 1 Schematic drawing of a protruded and a retracted hornerid polypide with atrial and vestibular spaces highlighted. Arrows indicate positions of the membranous sac attachments to the skeleton

In some Cheilostomatida the lack of ECM and coelothelium in the zooid lining adjacent to the skeleton is well-documented (Mukai et al., 1997 and references within; Shunatova & Tamberg, 2019; Shunatova et al., 2021), even though cell contacts in the epidermis are preserved (Shunatova & Tamberg, 2019, Figure 13b). In ctenostomates, too, the endocyst appears devoid of ECM and peritoneum (e.g., Schwaha & De Blauwe, 2020), although without a TEM study the state of cell continuity and cell junctions remains unknown in this group. By contrast, in all examined phylactolaemates the endocyst retains ECM, coelomic lining and typical cell junctions (Mukai et al., 1997, Figures 11 and 12; Shunatova & Tamberg, 2019, Figure 4e).

Borg (1926a) identified four components of a cyclostome body wall: the cystid, the terminal membrane, the vestibular walls and the tentacle sheath. The living part of the cystid—the endocyst—is harder to delineate in cyclostomes than in other bryozoans because the typical coelomate body wall composition is modified in this clade. The epidermis remains in association with the skeleton while the ECM and coelothelium have detached and exist independently as the membranous sac (Nielsen & Pedersen, 1979). Thus, the main body cavity is split by the membranous sac into two parts: the exosaccal cavity outside, and the endosaccal cavity (true coelom) inside (Figure 1).

Bryozoans in the family Horneridae are free-walled cyclostomes, characterised by two delicate layers of living tissue covering the topological exterior of their calcified colonial skeletons. The tissue layers are separated by a hypostegal cavity, which Borg (1926a, 1926b) considered as coelomic based on histological examinations. This view remained dominant until Nielsen and Pedersen (1979), working with the fixed-walled articulate genus *Crisia*, demonstrated that the exosaccal cavity was not coelomic in nature. Without studying it directly, the authors predicted that in free-walled species the hypostegal cavity is also non-coelomic. Here, we examine this prediction and explore variability of epithelial and non-epithelial structures of the body wall and exosaccal cavity. This study is a companion piece to Tamberg et al. (2021), it is based on the same material, and examines the same species with light and electron microscopic methods, but with the emphasis on various epithelia of the body wall.

2 | MATERIAL AND METHODS

We examined four hornerid species from two genera: *Hornera robusta* MacGillivray, 1883, *Hornera* sp. 1, *Hornera* sp. 2 and Horneridae gen. sp. 3. Material and methods in this study mostly overlap those in Tamberg et al. (2021). For more details on sampling and processing please consult this publication.

Three *Hornera* species, *H. robusta*, *H.* sp. 1 and *H.* sp. 2, were collected from the mid-continental shelf off Otago, New Zealand (90 m depth, 45° 47.89' S, 170° 54.5' E). *Hornera* sp. 2 was also collected

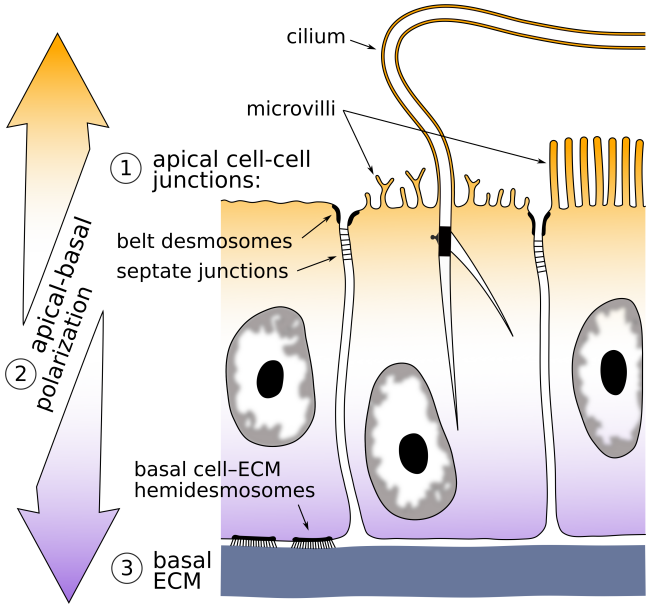

FIGURE 2 Schematic drawing of a fragment of a generalised epithelium showing three major identifying characters: cell cohesion, apical–basal polarisation and basally located extracellular matrix (ECM)

near Stewart Island (58 m and 77 m; 46° 54.87′ S, 168° 13.06′ E and 47° 07.70′ S, 168° 10.79′ E respectively). The last species, Horneridae gen. sp. 3 was obtained near the subantarctic Snares Islands (151 m; 47° 43.20′ S, 167° 1.44′ E).

At least 12 colonies of each species were fixed at sea, immediately after collection. In addition, living colonies of *H. robusta* and *H.* sp. 2 were taken to the laboratory and kept in flow tanks in an isothermic room at ~13°C, where they were left to recover from dredging for 3–8 days. Throughout this time the animals were constantly supplied with a mixture of natural particles and cultured algae and periodically examined with a dissecting microscope. Feeding colonies were relaxed with an isotonic solution of magnesium chloride (~7.5%) mixed 1:1 with sea water and fixed.

For semi-thin and ultrathin sections, samples were fixed with 2.5% glutaraldehyde solution in 0.1 mol L^{-1} PBS supplemented with sucrose to reach 990 mOsmol, and processed using standard TEM protocols. Material was rinsed in 0.1 mol L^{-1} PBS with sucrose (990 mOsmol), decalcified with 10% buffered EDTA and transferred into 1% OsO_4 for 1.5 h. After osmication, the material was washed, dehydrated through a graded ethanol series and pure acetone, and embedded in Embed 812 epoxy resin. Sectioning was done with a diamond knife on a Leica EM UC7 ultramicrotome. Resulting series of semi-thin sections (0.8 or 1-μm thick) were stained with toluidine blue and imaged with a light microscope. Ultrathin sections (80–90 nm) were stained with uranyl acetate and lead citrate and imaged with a JEOL 2200FS electron microscope. In addition to complete sets of combined semi-thin and ultrathin serial sections (≥5 series per species, ≥5 polypides per series), described in Tamberg et al. (2021), incomplete sets and individual sections were also used in this study.

Tiled montages were aligned using the Etomo element of IMOD software (RRID:SCR_003297; Kremer et al., 1996). All measurements were made from microphotographs using Inkscape 0.92 (RRID: SCR_014479; Inkscape project, 2017).

3 | RESULTS

The general organisation of the body wall of all studied species is relatively uniform, but a number of ultrastructural differences sets our studied hornerids apart from other described cyclostomes. In particular, we did not find orificial muscles, and some of the keystone epithelial traits (or even the epithelial layers themselves) are missing in various body wall elements. Table 1 summarises epithelial cell types and traits from this study and Tamberg et al. (2021), a companion study where we characterised the polypide, that is, tentacles, lophophore base, digestive system and funiculus, of these species.

3.1 | Terminal membrane and vestibular wall

The terminal membrane forms the frontal wall of a hornerid autozooid, the boundary separating it from the external environment. This delicate cuticular membrane stretches across the skeletal aperture, often with a noticeable depression towards the orificial opening (Figure 3), which can expand from a near-perfect closure to almost the internal diameter of the zooid tube, accommodating polypide protrusion.

Contrary to expectations, the terminal membrane of all studied hornerids is often represented by a single cuticle layer devoid of a continuous epithelial layer, although numerous isolated underlying cells are also present (Figure 3c). We rarely observed neighbouring cells touch, and did not find cell contacts or ECM. The cytoplasm of these cells is somewhat electron-lucent and contains a typical set of organelles but no distinguishing features. The musculature of the terminal membrane is restricted to some fine muscle strands, which we interpret as potential vestibular dilators (longitudinal ectodermal muscles). They were occasionally found on the sections near the terminal membrane, although we never saw their insertion points. We also did not see a defined orificial sphincter musculature in TEM or semi-thin preparations of any of the studied hornerid species, even though the orifice is usually closed when the polypide is retracted.

The cuticle of the terminal membrane folds inward at the orifice and extends into the vestibulum, becoming the lining of the vestibular wall (Figures 3 and 4). At the periphery of the terminal membrane this unbroken cuticular layer also extends over the peristome edge and onto the surface of the colony. Often, but not always, the outer colony covering has a more-complete cell layer underneath the cuticle (see below).

The vestibulum of the zooid continues proximally from the orifice to the atrial sphincter. The distal portion of the vestibular walls is similar to the terminal membrane, that is, partly naked cuticle with

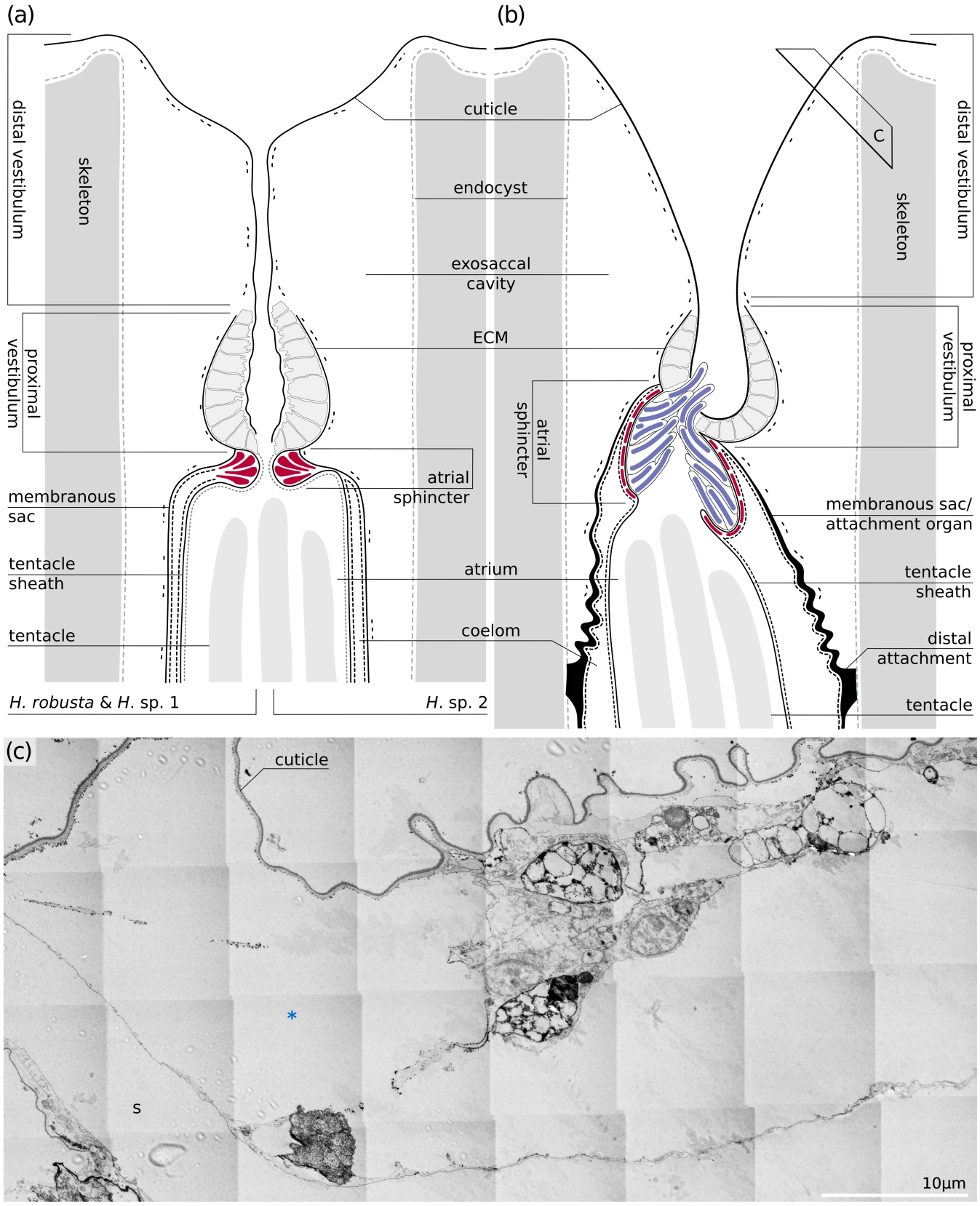

FIGURE 3 Distal portion of the zooids. (a, b) schematic drawings of the distal portion of the zooid in *Hornera* spp. (a) and Horneridae gen. sp. 3 (b). Position of (c) is depicted with a black frame. (c). Obliquely transverse section through the terminal membrane of Horneridae gen. sp. 3

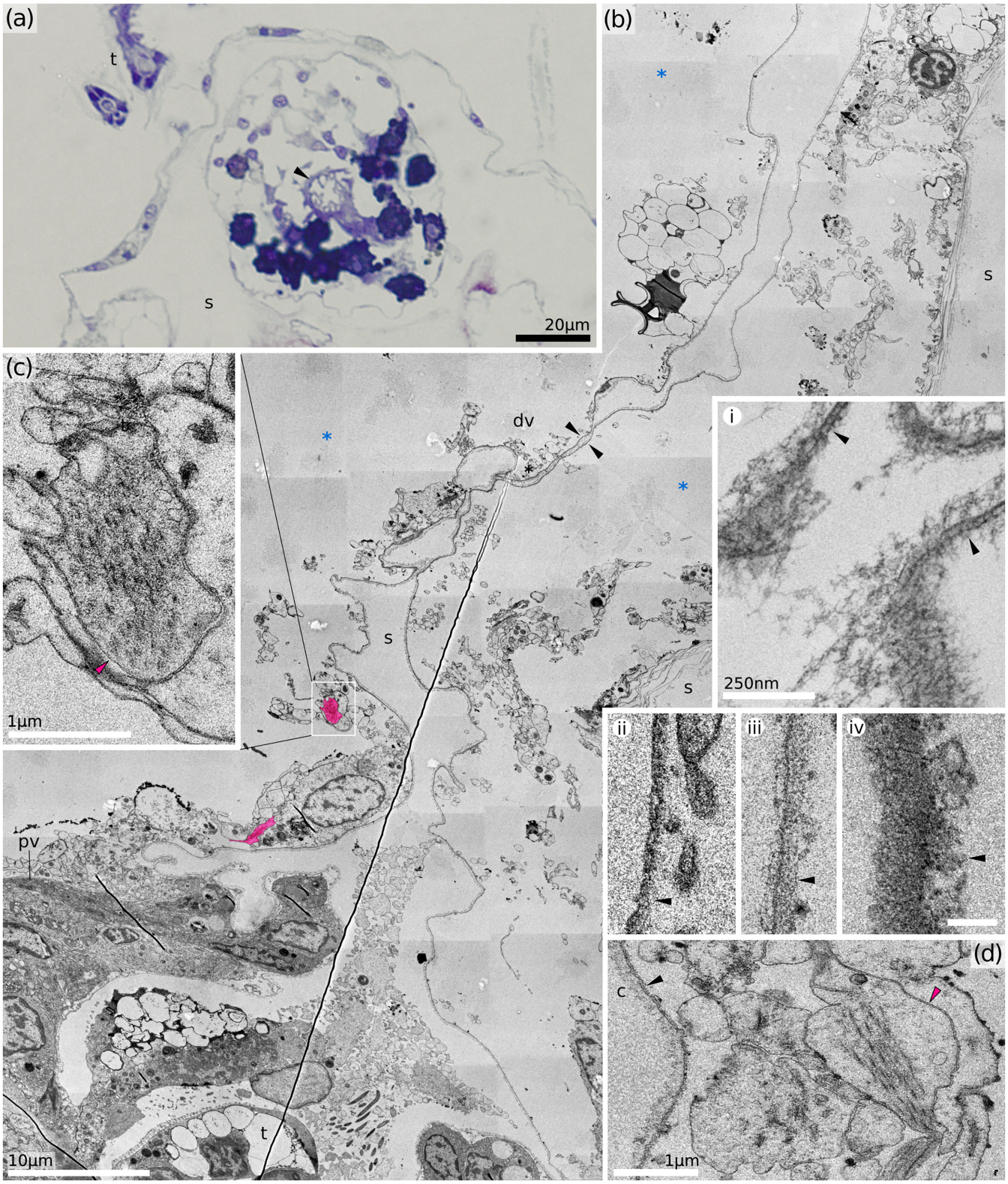

FIGURE 4 Distal part of vestibulum. (a) Transverse section of the upper vestibulum in *H.* sp. 2. (b) Longitudinal section through distal portion of a partially retracted zooid (*H. robusta*). Note the tentacle tip visible at the very bottom, which is a result of incomplete polypide retraction during fixation. In fully retracted polypides the tentacles are never seen distally of the atrial sphincter. Putative longitudinal ectodermal muscles are tinted red. Insets demonstrate variability of vestibular cuticles: i – *Hornera robusta*, ii – *H.* sp. 1, iii – *H.* sp. 2, iv – Horneridae gen. sp. 3; scale bars identical for ii, iii and iv, 200 nm. (c, d) details of the putative longitudinal ectodermal muscles. *c, cuticle; dv, distal vestibulum; pv, proximal vestibulum; s, skeleton; *, exosaccal cavity; black arrowheads, vestibular cuticle (in all cases the arrows point at the inner surface of the cuticle); red arrowheads, putative vestibular dilator muscles*

TABLE 1 Epithelial types of the studied hornerids

Type/location	Continuity	ECM	Cell type	Apical structures; Microvilli	Apical structures; Cilia	Cuticle	Shape
1. Epidermis							
Tentacles	+	+	Plain	+	+/−	Microvillar	Cuboid
Tentacle sheath	+	+	Plain	−	− (free basal bodies)	−	Squamous
Proximal vestibular wall	+	+	Plain	−	−	Smooth	Cylindrical/irregular
Distal vestibular wall, orifice, terminal membrane	Partial	−	Plain	−	−	Smooth	Squamous/irregular
Zooidal endocyst	Partial	−	Plain	−	−	−	Squamous
Outer colonial wall	partial	−	plain	−	−	Smooth	Irregular, squamous
2. Gut epithelium							
Pharynx	+	+	Myoepithelial	+	+	Microvillar	Cylindrical
Cardia	+	+	Plain	+	−	−	Cuboid
Caecum	+	+	Plain	+/−	−	−	Cylindrical
Pylorus	+	+	Plain	+	+	−	Cuboid
Rectum	+	+	Plain	−	−	−	Cuboid
3. Coelothelium							
Tentacles	+	+	Myoepithelial/plain	−	−	NA	Cuboid
Lophophore/ring canal	+	+	Plain	−	−	NA	Cuboid/squamous
Membranous sac	+	+	Plain	−	−	NA	Cuboid/squamous
Gut	+	+	Plain	−	−	NA	Cuboid/squamous

occasional (possibly non-epithelial) cells on its inner surface. In the retracted polypides of *Hornera*, the vestibular space has the shape of a narrow cylinder, measuring only ~5 × 15 μm in diameter (Figure 4a, b), and lined with folded cuticle. In Horneridae gen. sp. 3 the vestibular space may be cylindrical or funnel-shaped, starting at the same width as the aperture and narrowing towards the atrium. In the latter case, the terminal membrane cannot be distinguished from the vestibular wall. In addition, the cells underlying the terminal membrane in this genus are more numerous compared to all three *Hornera* species.

The cuticle of the terminal membrane and vestibulum varies in thickness and composition between hornerid species, from ~120 nm in *H*. sp. 2 to ~170 nm in *H. robusta* and up to ~300 nm in Horneridae gen. sp. 3. The cuticle is non-uniform in composition, with an apparently three-layered baseline condition (Figure 4i–iv). In all studied species of *Hornera* the top layer is made of loose vertically oriented fibrillar material, whereas Horneridae gen. sp. 3 has a more compact top layer. A thin but well-defined electron-dense midlayer and irregular fibrillar bottom layer are common in all studied hornerids. The uppermost layer is almost glycocalyx-like, missing in *H*. sp. 1 and varying from ~55 nm in *H*. sp. 2 to ~110 in *H. robusta*. In Horneridae gen. sp. 3 the upper layer is denser and reaches ~105 nm in thickness. The medial dark layer is more stable in thickness (~17 nm in *H*. sp. 2 and ~35 nm in all other species). On tangential sections of terminal membrane cuticle in *H. robusta* we found circular profiles, reminiscent of "trapped" microvilli (Figure 4i). The innermost layer is also variable in thickness (from ~30 nm in *H. robusta* and ~50 nm in *H*. sp. 1 and *H*. sp. 2 up to ~150 nm in Horneridae gen. sp. 3).

In the proximal portion of the vestibulum, the body wall includes a distinct epithelial cellular component underlying the cuticle (Figures 5 and 6). The proximal vestibular wall is made of typical epidermis, in its proximal part resting on the basement membrane (tinted blue in Figure 5a,b). In *Hornera*, the proximal vestibulum has the shape of a folded cylinder (Figures 3a and 5c), whereas in Horneridae gen. sp. 3 it is more spacious and has no folds, resembling a deep bowl (Figure 6a). In retracted polypides of *Hornera*, proximal vestibular cells are often tall (up to 15 μm), with unevenly bulging apical tips (Figure 5c). When the polypide is protruded, many of these cells become more flattened (2–6 μm; Figure 6c). The proximal vestibular cells have no elaborations of the cell membranes, or any apical structures. Nuclei are predominantly found in the apical, not basal position. In Horneridae gen. sp. 3, apical surfaces are smooth and flat underneath an unfolded cuticle (Figure 6a). In all species, however, vestibular cells bear signs of active biosynthesis: in older cells we found numerous enlarged cisternae of rER, while younger cells had multiple, large and deeply curved Golgi complexes (≥10 dictyosomes in a stack; Figure 6b).

In many cases, we observed a conglomerate of non-epithelial cells and/or non-cellular material in the distal portion of the polypide,

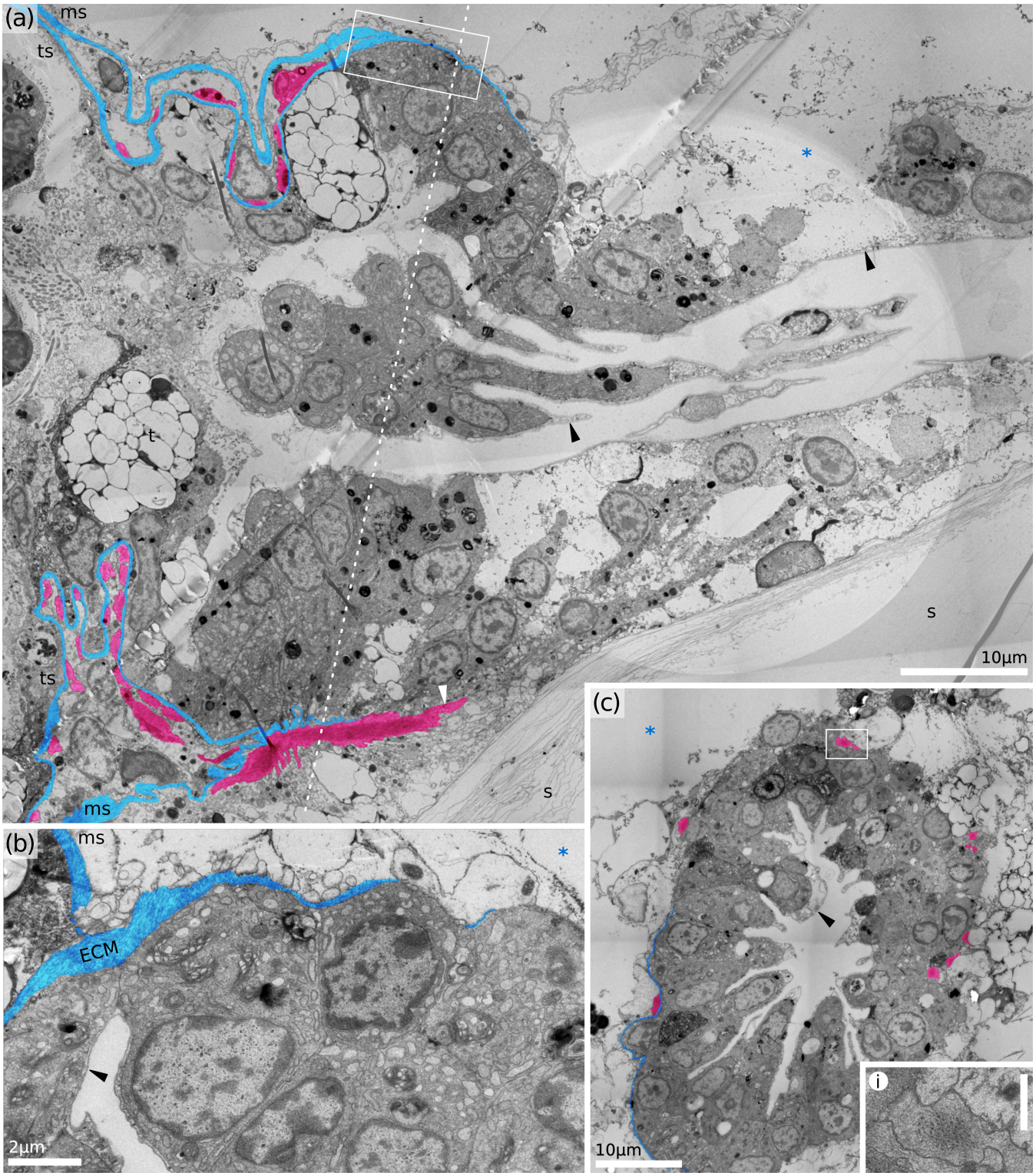

FIGURE 5 Proximal part of vestibulum in *Hornera robusta* (retracted polypide). (a) Longitudinal section. (b) Close-up of the proximal edge of vestibulum, showing ECM of the membranous sac joining ECM of the vestibulum. Note enlarged cisternae of rER. (c) Cross-section of the proximal vestibulum. Inset demonstrates longitudinal muscle of the proximal vestibulum (scale bar 1 µm). ECM tinted blue, atrial sphincter muscles and a putative vestibular dilators tinted red. *ECM, extracellular matrix; ms, membranous sac; ts, tentacle sheath; s, skeleton; *, exosaccal cavity; black arrowheads, vestibular cuticle, white arrowhead, putative vestibular dilator*

occupying the exosaccal cavity between the terminal membrane and the lower vestibulum. Similar, but presumably strictly cellular, agglomerations were recently reported as the 'upper cell complex' in crisiids (Nekliudova et al., 2021). In addition, loosely arranged cells are located on the exosaccal side of the proximal, epithelialised portion of the vestibular wall. We did not detect any cell contacts, and

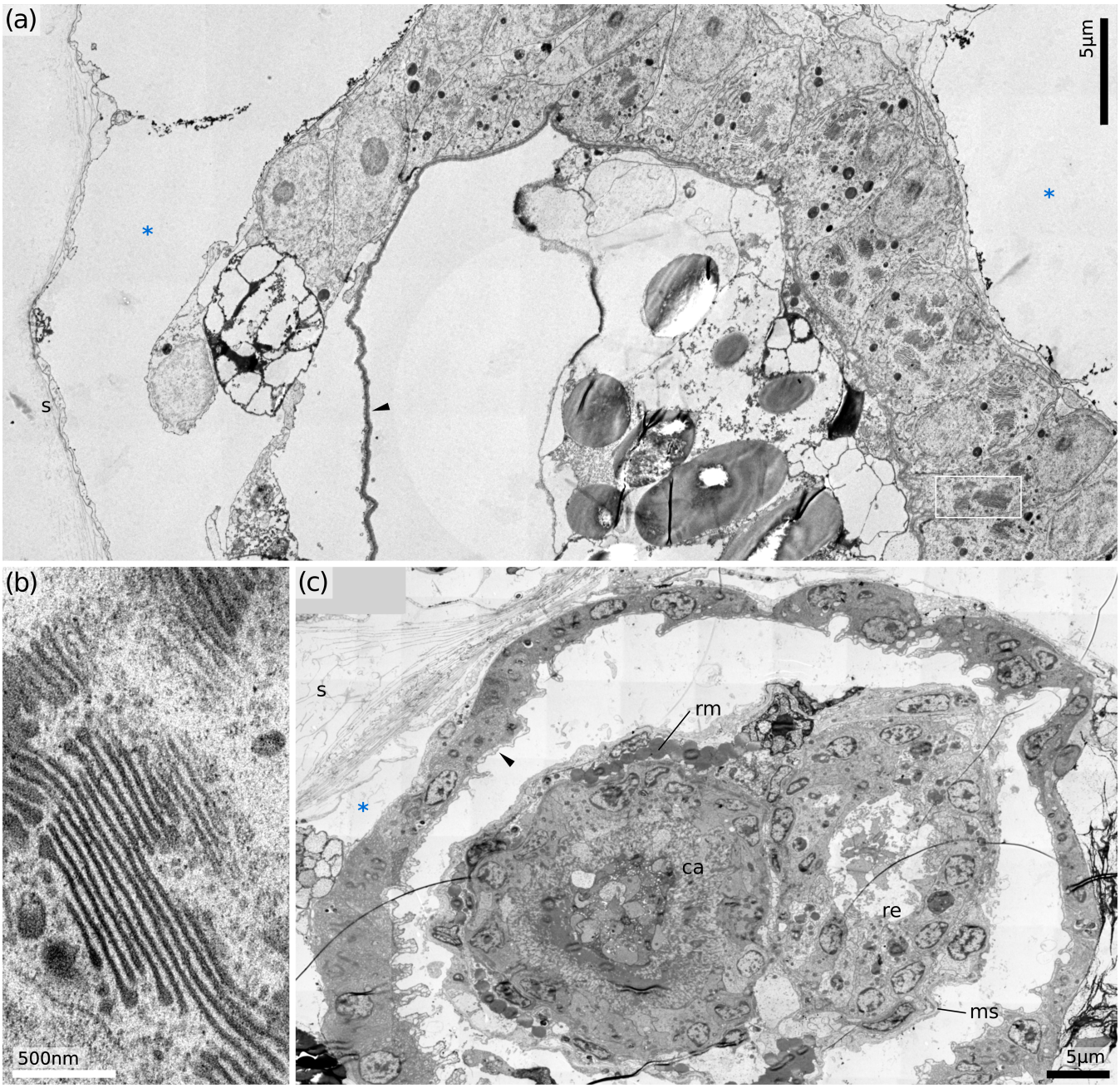

FIGURE 6 Proximal part of vestibulum. (a) Cross-section of Horneridae gen. sp. 3 (retracted polypide). (b) Golgi fields in vestibular cells of Horneridae gen. sp. 3 (area similar to black frame in A). (c) Cross-section of the *H.* sp. 2 (protruded polypide). *ca, cardia (downward gut branch); ms, membranous sac; re, rectum (upward gut branch); rm, retractor muscle; s, skeleton; *, exosaccal cavity; black arrowheads, vestibular cuticle*

ultrastructurally these cells resemble loose epidermal cells of the terminal membrane and the distal part of the vestibulum. Some of these cells appear to stretch towards the zooid walls, which implies similarity with 'mesothelial' cells reported by Nekliudova et al. (2021).

In all examined *Hornera* species we also found some delicate longitudinal musculature associated with the proximal part of the vestibular wall (tinted red on Figures 4 and 5). We were unable to locate the hemidesmosomes and thus the attachment points of these muscles. They could either be specific to vestibular wall, or extend beyond it towards the terminal membrane (i.e., be vestibular dilators), or both.

The proximal vestibulum could be misinterpreted as an atrial sphincter, especially with light microscopy, due to its substantial appearance. However, the true atrial sphincter is located more proximally.

3.2 | Atrial sphincter

The atrial sphincter is a muscular ring or cylinder that separates the vestibular space from the atrium in the retracted polypide (Figures 3a,

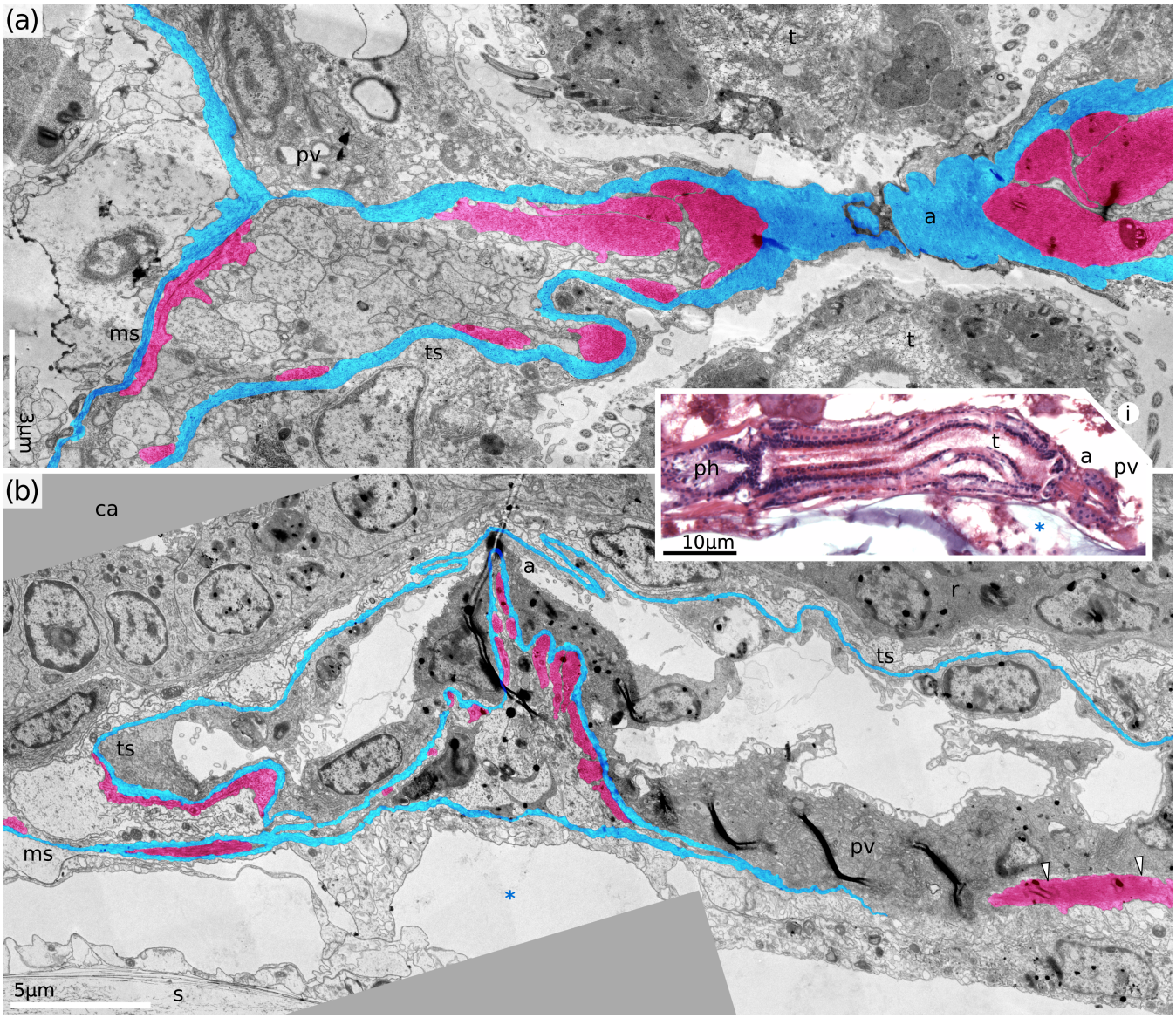

FIGURE 7 Atrial sphincter in retracted and protruded polypides. (a) Tangential longitudinal section of atrial sphincter in *H. robusta* (retracted polypide, distal direction on the right). Note the tentacle protruding into the vestibular space due to incomplete retraction of the polypide during fixation. Inset shows longitudinal section of the same species providing context and interrelationship between proximal vestibulum and atrial sphincter. (b) Longitudinal section of *H.* sp. 2 (protruded polypide). *a, atrial sphincter; ca, caecum; ms, membranous sac; ph, pharynx; pv, proximal vestibulum; t, tentacle; ts, tentacle sheath; s, skeleton, *, exosaccal cavity*

b, 7 and 8). Both spaces are continuous with the external environment and cannot be considered internal cavities of the zooid as they are lined with external body walls. In addition, the atrial space is temporary in nature and disappears when the polypide is protruded.

The proximal end of the vestibular wall joins the membranous sac and the tentacle sheath of the polypide in a Y-shaped junction (Figure 5a,b). Immediately below the merging point with the vestibular wall, the tentacle sheath forms a folded cylinder which houses the atrial sphincter. Numerous circular muscles of the sphincter are attached to the ECM of the tentacle sheath (Figure 7). In both, the retracted and protruded polypides, the area of the atrial sphincter contains no lumen. Distally all space is occupied by muscle cells (both their contractile portions and the somata), proximally by the coelothelium (Figures 7 and 8). In *H. robusta*, the atrial region has the simplest organisation, in *H.* sp. 2 it has an additional complication: the ECM of the tentacle sheath just below the atrial sphincter merges briefly with that of the membranous sac for the second time (Figures 3a and 8b). Thus, the atrial sphincter appears enclosed by a complete layer of ECM: a loop in a longitudinal section or torus in 3D.

In all three studied *Hornera* species the atrial sphincter region is only up to 10 µm tall (see Figure 8i) and located terminally at the proximal-most point of the vestibulum. In Horneridae gen. sp. 3 the atrial region is significantly taller (50–70 µm) and the atrial opening does not coincide with the bottom of the vestibulum (Figure 9a).

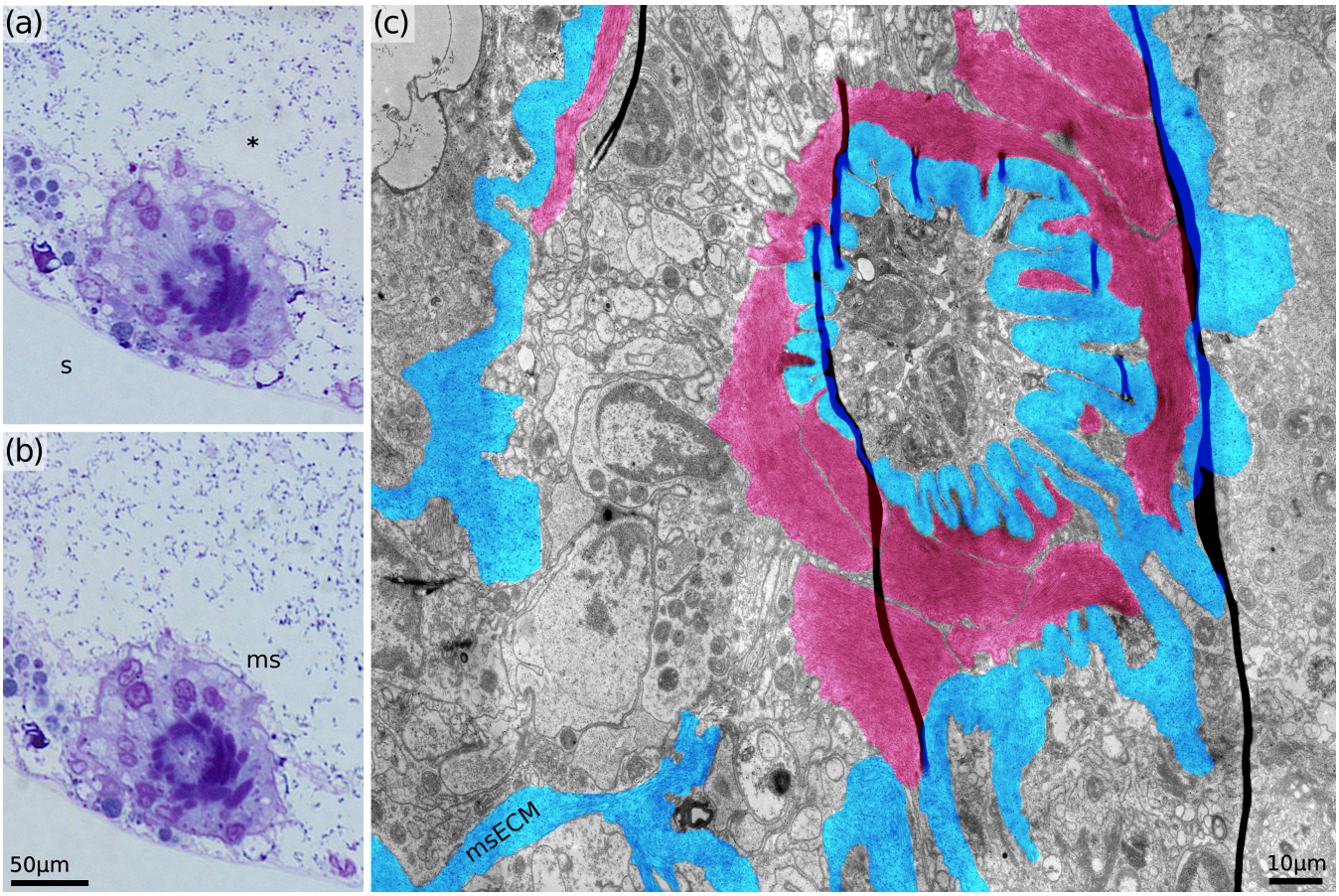

FIGURE 8 Transverse view of the contracted atrial sphincter in two *Hornera* species. (a,b) Consecutive sections of *H.* sp. 1. (c) Section of *H. robusta* (distal direction to the right). Musculature tinted red, ECM tinted blue. *ms, membranous sac; msECM, extracellular matrix of the membranous sac; s, skeleton; white arrowhead, putative vestibular dilator muscle; *, exosaccal cavity*

Instead, it is located ~10 µm more distally, attaching to one of the sides of the bowl. Epidermal cells of the atrial area also differ strikingly between genera. In *Hornera* the epidermis is composed of typical squamous or cuboid cells (e.g., Figure 7b), whereas in the other genus the outer atrial epidermis is strongly modified (compare with Figure 9). Epidermal cells are unusually large (some measuring 15–20 µm in apical-basal direction) and contain several homogeneous inclusions which take the form of long and flexible cylindrical rods (Figure 9). We provisionally interpret these structures as mucoid secretions based on their homogeneous, relatively electron-dense appearance. In addition, we note numerous shudder marks or tears left by the ultratome knife during sectioning, which suggests relatively poor resin infiltration compared to other tissues. The diameter of these rod-like inclusions varies around 3.5 µm, while their length may reach 50 µm. The orientation of the rods is predominantly proximal-distal, running along the zooidal axis (Figure 9). In the cytoplasm near the inclusions, we found poorly preserved vesicle profiles which could be enlarged cisternae of ER. Although the rod-bearing cells originate in the atrial region, their distal tips protrude upwards through the atrial opening and into the vestibulum (Figure 9). The voluminous agglomeration of the rod-bearing cells effectively seals the entrance into the atrium, so the atrial musculature is never contracted as tightly as in three examined *Hornera* species.

3.3 | Membranous sac

The membranous sac is a mostly free, elongated, sock-like structure which encloses the polypide. It originates at the same point where the vestibular wall joins the tentacle sheath and continues past the proximal tip of the gut, following the funiculus (Figures 1 and 10a). It is supplied with fine muscles (Figures 8 and 10) and terminates blindly at the origin of the funiculus (see Tamberg et al., 2021). In *Hornera* species, the membranous sac is attached to the cystid wall at only two points: at the origins of the retractor muscles and the funiculus (Figure 11). In Horneridae gen. sp. 3 there is also a well-developed atrial attachment organ which anchors the membranous sac to the skeleton in the distal portion of the zooid (Figure 12). In this genus the ECM of the membranous sac slopes down from the origin point above the atrial sphincter towards anchoring sites in the form of a circular diaphragm, limiting body fluid circulation between the distal and proximal parts of the exosaccal cavity. Attachment zones are

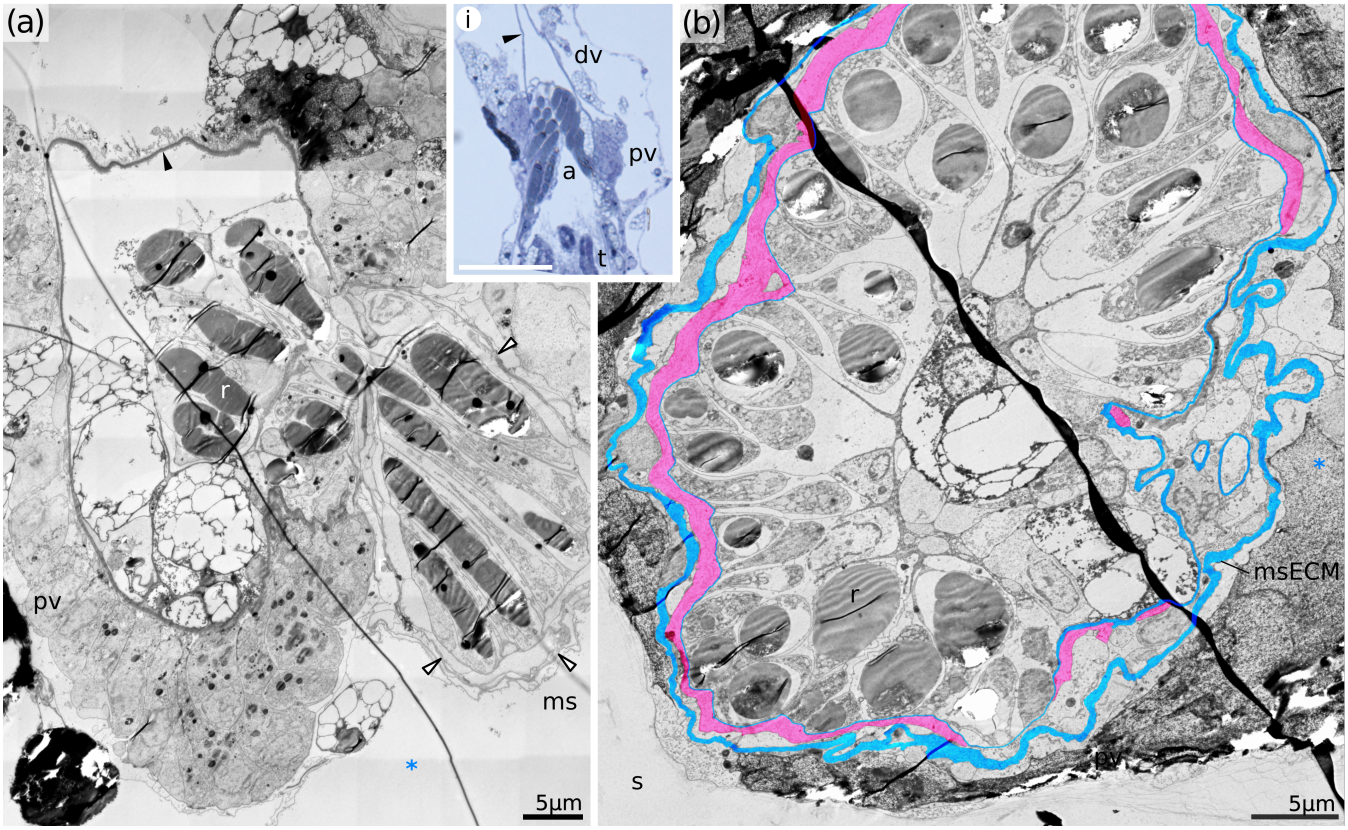

FIGURE 9 Atrial sphincter in Horneridae gen. sp. 3. (a) Longitudinal section of the proximal vestibulum showing tangential cut through the atrial sphincter. Inset demonstrates interrelationships between distal and proximal vestibulum and atrial sphincter (scale bar 50 µm). Note modified epidermal cells with rod-like inclusions protruding distally into the proximal vestibulum. (b) Cross-section through the closed atrial sphincter in Horneridae gen. sp. 3 w ith structural elements coloured blue (ECM) and red (atrial sphincter muscles). Note modified epidermal cells containing electron-dense rods. *a, atrial sphincter; dv, distal vestibulum; ms, membranous sac; msECM, ECM of the membranous sac; pv, proximal vestibulum; r, rod-like inclusions of the epidermal cells; s, skeleton; t, tentacle; *, exosaccal cavity; white arrowheads, ECM of the membranous sac*

represented by 7–9 individual ligaments evenly spaced around the zooid chamber (Figure 12b,c). All ligaments measure approximately 18–20 µm in both the proximal-distal direction (Figure 12d) and laterally (Figure 12e). Gaps between ligaments are of similar size. Numerous muscle cells are embedded in the ECM near the ligaments and elsewhere in the attachment organ (Figure 12d,e). This distinguishes them from other muscles of the membranous sac which are never embedded in the ECM (Figure 10).

The anchoring structures, that is, the ligaments, of the membranous sac show a striking uniformity across the species: in all cases specialised epidermal cells of similar morphology (tendon cells) are interposed between the ECM of the membranous sac and the skeletal wall (Figures 11 and 12). The nucleated somata of a tendon cell are displaced sidewise, like the handle of a frying pan, whereas the central thin portion is sandwiched between ECM and the skeleton. The interfaces have numerous hemidesmosomes, densely packed on the apical and basal cell membranes. Bundles of tonofilaments (10–13 nm thick) originate from the hemidesmosomes and traverse the cytoplasm (Figures 11 and 12e; Figure 8b in Tamberg et al., 2021). An irregular arrangement of hemidesmosomes and tonofilaments, together with pale cytoplasm, gives these cells an unhealthy appearance. The ECM in contact with the ligament may be slightly thickened, but is otherwise unmodified.

The origins of retractor muscles have particularly large footprints in all examined species. The ligaments in this area comprise several adjacent tendon cells. The latter are joined by septate junctions, which, notably, were the only example of cell junctions observed in the endocyst during this study (Figure 12f).

The ECM and the coelothelium of the membranous sac transition seamlessly into those of the tentacle sheath (Figure 8). The peritoneal lining is made of thin, delicate cells with few cell contacts and no ciliation. The peritoneal cells can occasionally penetrate the ECM they rest against and make contact with other cell layers: the epidermis of the tentacle sheath as well as the lining of the lophophore coelom. The musculature of the membranous sac is represented by predominantly diagonal (and/or possibly circular) myoepithelial cells located on the endosaccal surface underneath the coelomic epithelium (Figures 10a,b and 14b). In *H.* sp. 2 and Horneridae gen. sp. 3, we also found some longitudinal muscles in the membranous sac near the origins of the retractor muscles.

We were surprised to find that the outer (exosaccal) surface of the membranous sac is often covered with squamous cells and smaller

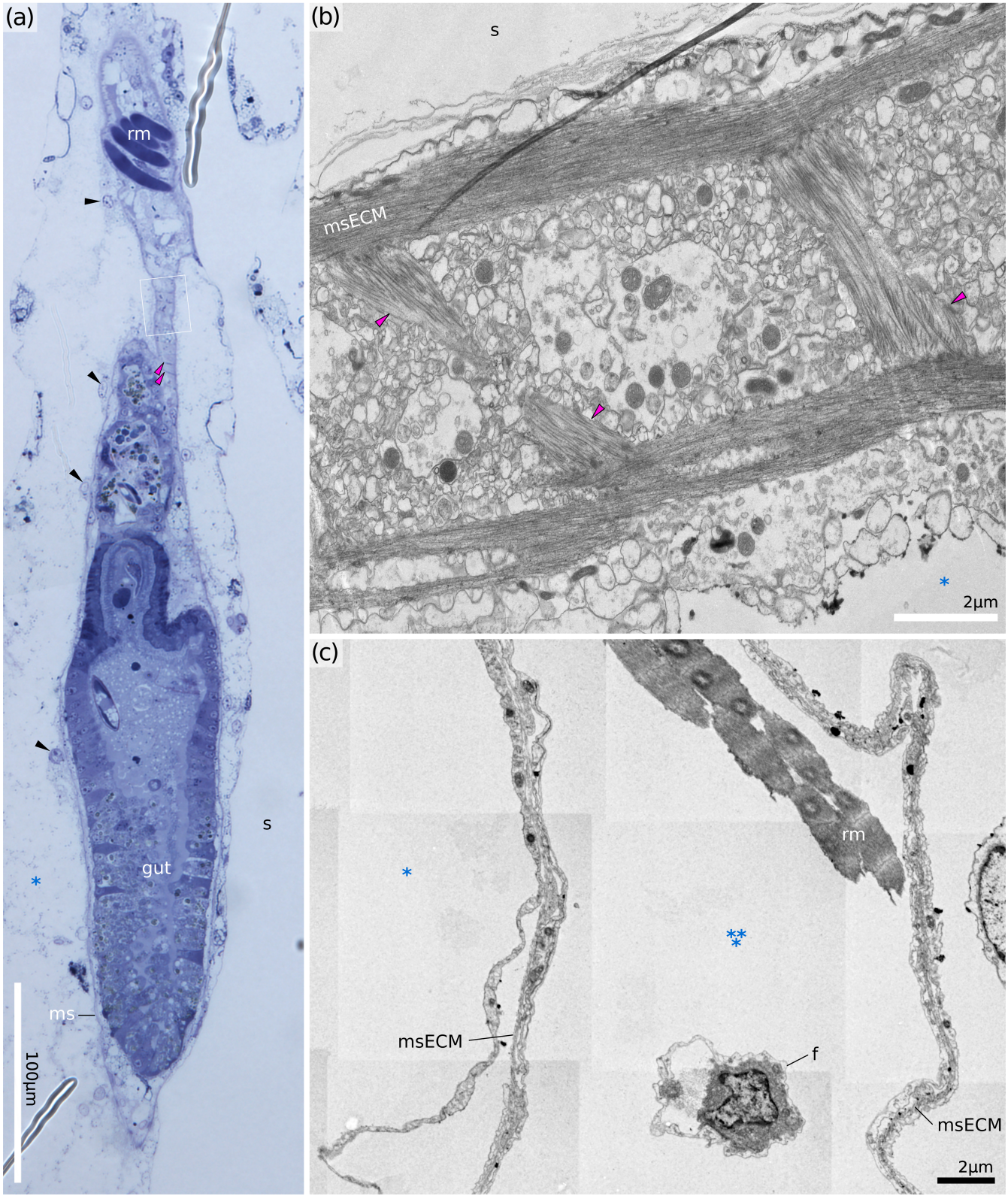

FIGURE 10 Membranous sac of *H. robusta* (retracted polypides). (a) Longitudinal section of the zooid. (b) Tangential section of the membranous sac showing diagonal muscles and ECM, showing area similar to the white frame in (a). (c) Longitudinal section of the zooid proximal of the polypide (*H.* sp. 2, protruded polypide). *f, funiculus; ms, membranous sac; msECM, extracellular matrix of the membranous sac; rm, retractor muscles; s, skeleton; black arrowheads, extraepidermal cells on the outer surface of the membranous sac; red arrowheads, diagonal musculature of the membranous sac; *, exosaccal cavity, ***, trunk coelom*

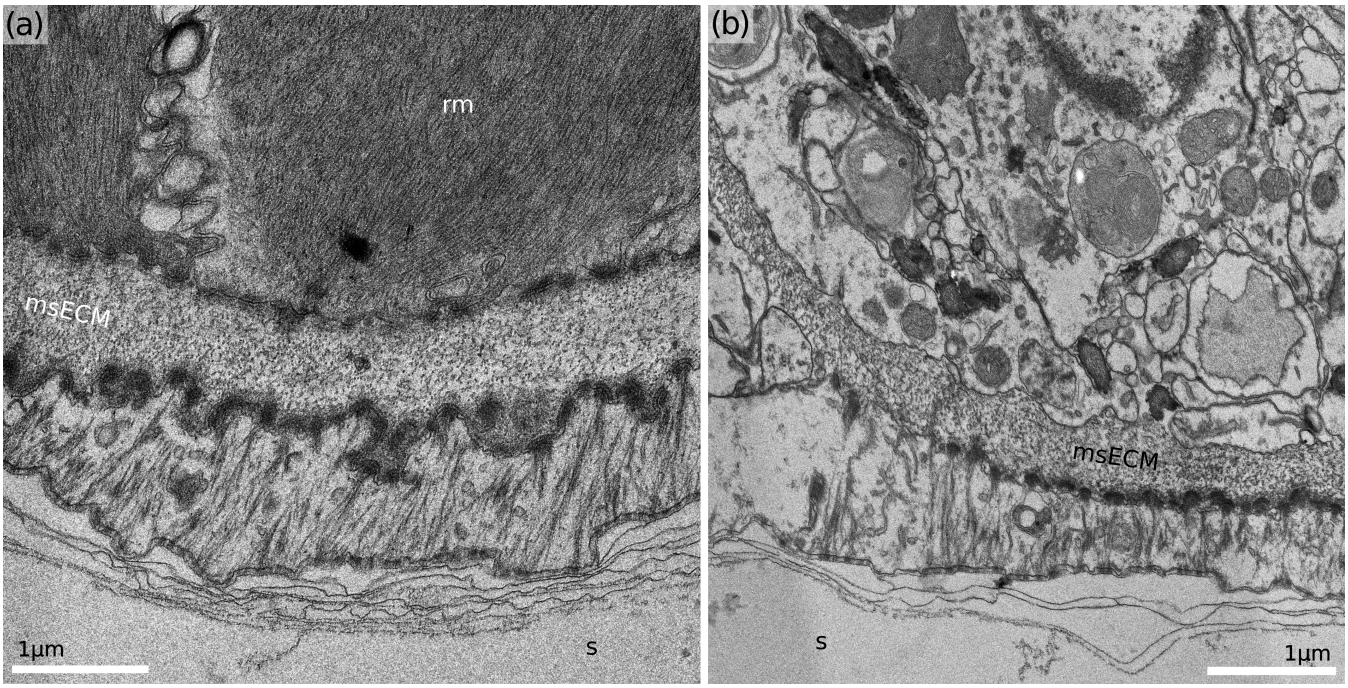

FIGURE 11 Proximal membranous sac attachments in *Hornera* sp. 2. (a) Cross-section of the retractor muscle attachment zone showing tendon cell interposed between the ECM and the skeleton. (b) Cross-section through the distal portion of funicular attachment footprint. Note the tonofilament-free portion of the cytoplasm of the tendon cell on the left. *msECM, extracellular matrix of the membranous sac; rm, retractor muscle; s, skeleton*

membrane contours (Figures 8 and 10). These cells do not form a continuous epithelial layer, but nevertheless are common and numerous (which contradicts expectations based on the detached mesoderm hypothesis of Nielsen & Pedersen, 1979). These cells usually have pale cytoplasm, sparse organelles (mostly ER, mitochondria and irregularly shaped vacuoles), but no unusual features which would indicate active biosynthesis or reveal cell polarisation direction. Some of these cells appeared to stretch between the outer surface of the membranous sac and the endocyst lining of the skeleton in retracted polypides (Figures 5a and 8b).

3.4 | Endocyst

Hornerids have a free-walled (=interior-walled) outer body wall configuration (Figure 13). In all examined species, the epidermal lining of the zooid walls continues outwards beyond the zooidal boundaries, over the peristome and onto the outer surface of the colony. Here, this cell layer becomes a component of the outer colonial body wall. Similarly, the exosaccal cavity of the polypide continues beyond the zooidal chamber and becomes the extrazooidal space on the topographical exterior of the colony, that is, the hypostegal cavity (Borg, 1926a, 1926b).

All studied species demonstrated consistent similarity in the organisation of the cellular lining of the skeleton. Both within a zooid and in the outer colonial wall, it is a single, often incomplete epidermal layer, unsupported by the ECM (Figures 13 and 14). This incompleteness is particularly clear in the inner lining of the zooid and is less common in the colonial walls. In the latter case, the outer layer of the double wall is additionally covered by a cuticle, which is continuous with the terminal membrane and resembles the latter in thickness and composition (Figure 13). The exosaccal cavity may contain extraepithelial cells apparently unattached to any surface. They have a rounded shape with slightly uneven contours, and an electron-dense cytoplasm (Figure 14b).

3.5 | Interzooidal pores

Adjacent zooidal tubes are connected in a number of places by circular interzooidal pores measuring ~7 µm in diameter (Figure 15). Hornerid autozooids contain numerous pores, often 50 or more (cf. crisiids with 4–8 interzooidal pores per zooid; Nielsen & Pedersen, 1979). Some pores are interzooidal (Figure 15a,b), while others connect to cancelli (Figure 15c), thin tubes running through the secondary skeleton which open into the hypostegal cavity (the hypostegal pores of Batson et al., 2021). The face of the pore is ornamented by an inward-facing fringe of skeletal spines partially occluding the opening. Regardless of position within the zooid (proximal or distal) the pore is occupied by a single pore cell (Figure 15). The nucleus is located within one of the connected zooidal chambers and the cytoplasm contains sparse ER cisternae and few small mitochondria. The rest of the cell volume is packed with numerous thin (6 nm in diameter) filaments (Figure 15). These filaments show a loosely regular arrangement, stretching from edge to edge and going over the center of the pore opening. In cross-section the resulting shape of the filament bundle resembles a lentil, about 5–7 µm thick, with the widest part corresponding to the midline

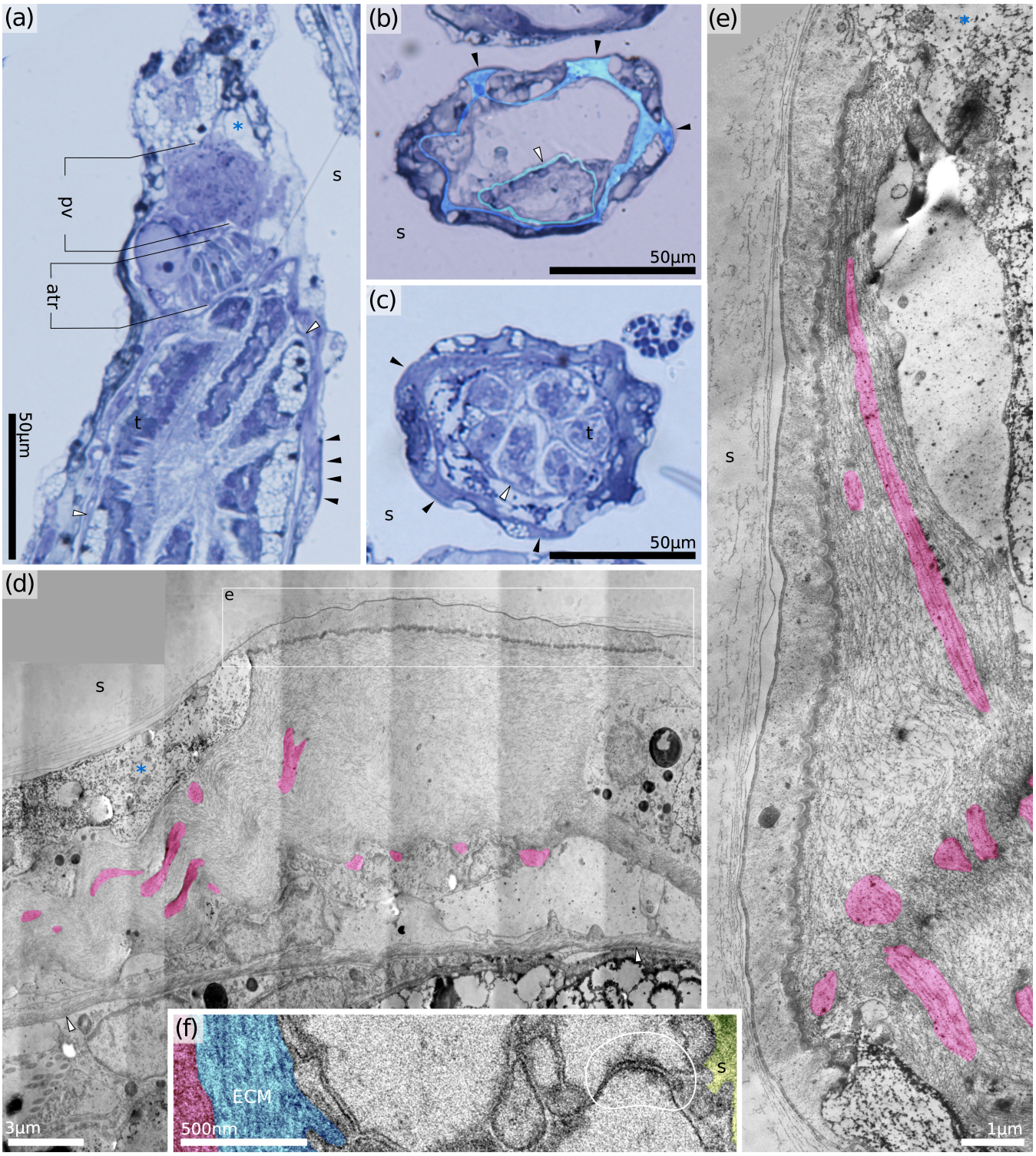

FIGURE 12 Distal attachment organ in Horneridae gen. sp. 3 (retracted polypide). (a) Oblique longitudinal section through the distal part of the zooid. (b,c) Consecutive cross-sections through the attachment organ just distal of the tentacle tips (b) and more proximally. Note only six tentacles visible at this level. (d) Longitudinal section through the attachment organ (proximal direction on the right, muscles tinted red). (e) Longitudinal section through the distal attachment showing the shape of the ligament and tendon cell (proximal direction up, muscles tinted red). (f) Cross-section through the retractor muscle attachment showing septate junctions (*H.* sp. 1). *atr, atrial sphincter; ECM, extracellular matrix; pv, proximal vestibulum; s, skeleton; t, tentacle; black arrowheads, proximal attachments of the membranous sac; white arrowhead, tentacle sheath; *, exosaccal cavity*

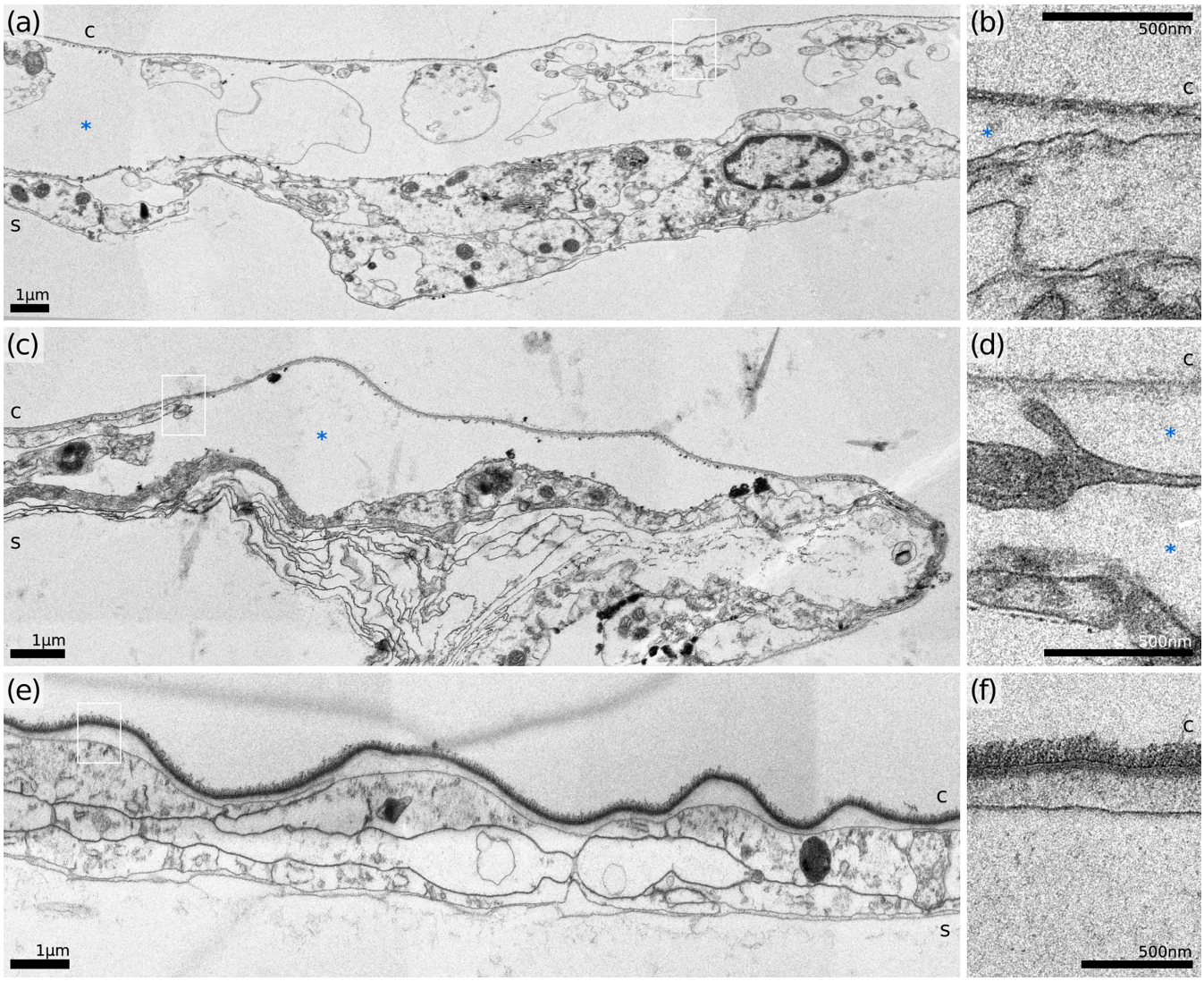

FIGURE 13 Outer (interior frontal) wall and cuticle details of three hornerid species. (a,b) *H.* sp. 1. (c,d) *H.* sp. 2. (e, f) Horneridae gen. sp. 3. Figures (b), (d) and (f) represent the areas similar to those in black frames on A, C and E, respectively. c, cuticle; s, skeleton; *, hypostegal cavity

of the pore. Although indentations in one of the surfaces are moderately common (Figure 15c), we saw no openings or channels through the pore cell itself in the studied species.

4 | DISCUSSION

4.1 | Organisation of the hornerid body wall in a wider context

The zooidal elements of the body wall in cyclostome bryozoans, namely the terminal membrane, vestibular and atrial walls, are anatomically complex despite their relatively simple appearance. These structures participate in polypide protrusion and retraction, including a hydrocompensatory role and protective sealing-off of the vestibular and atrial spaces (e.g., Ryland, 1970). The overall organisation of these regions is based on a conservative, cyclostome-specific foundation, but shows variability in structure, position and indeed presence/absence, of smaller characters.

The border between atrial and vestibular areas encompasses a three-way merging of the vestibular wall, membranous sac and tentacle sheath, as well as hosting the distal attachments of the membranous sac to the cystid wall (when present), the atrial sphincter, and the origins of vestibular dilators.

The organisation of the merging site of the tentacle sheath and membranous sac and location of the atrial sphincter is somewhat different among the examined hornerids compared to some other cyclostomes. Our findings agree with those of Borg (1926b), who reported that the atrial sphincter of *Plagioecia patina* is located at the distalmost edge of the tentacle sheath, just below the attachment organ and therefore more proximal than the merging point of the tentacle sheath and membranous sac. Even though species of *Hornera* have no distal attachment organs, and in Horneridae gen. sp. 3 the ligaments are displaced proximally from the atrium

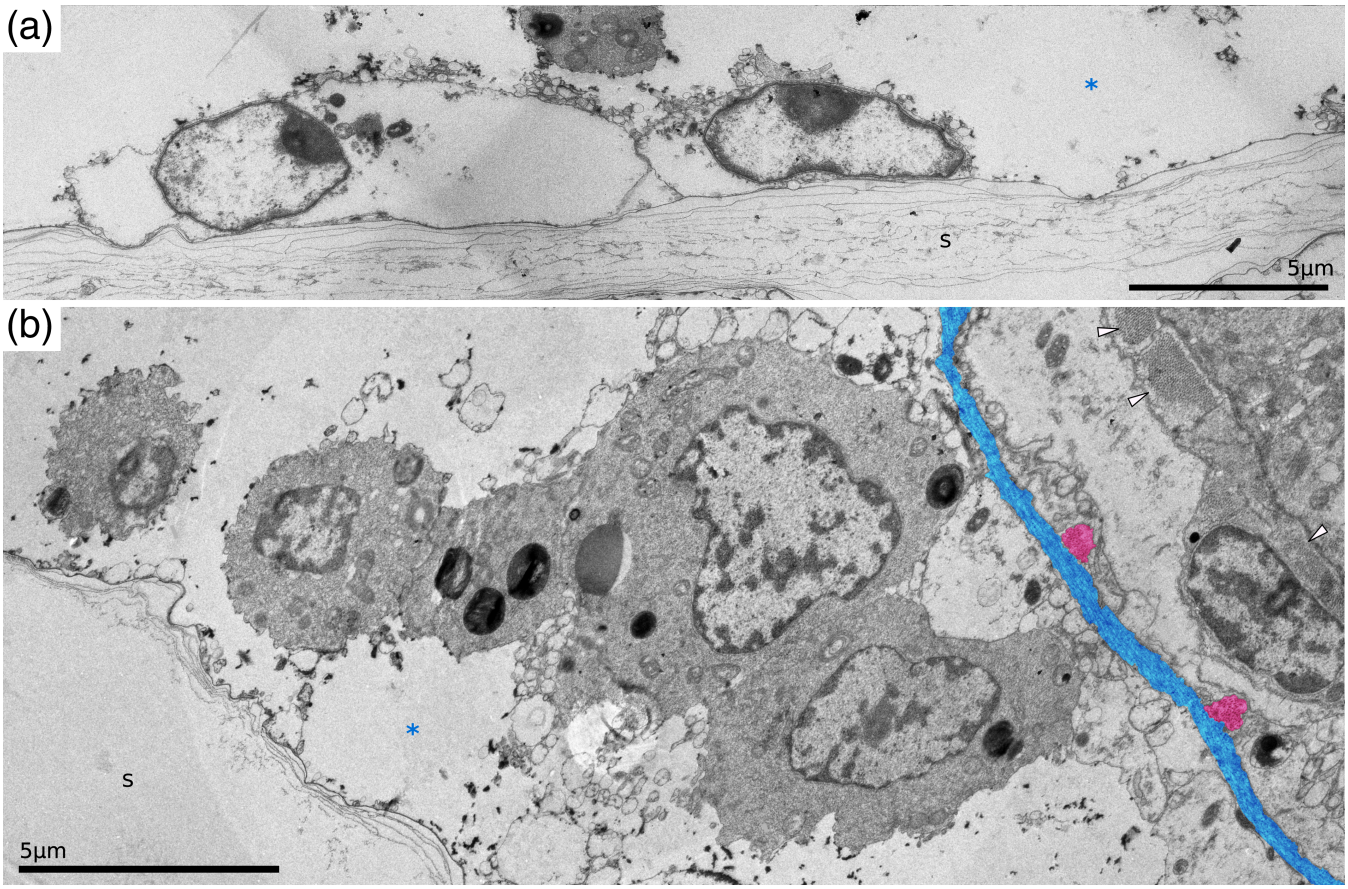

FIGURE 14 Details of endocyst in *Hornera robusta*. (a) Transverse section of the proximal zooid wall. (b) Longitudinal section through the zooid in the pharyngeal area. Note the lack of continuous epidermal cell cover of the endocyst and large oval extraepidermal cells in the exosaccal cavity. Elements of the membranous sac coloured blue (ECM) and red (circular musculature). *s, skeleton; white arrowheads, circular pharyngeal muscles; *, exosaccal cavity*

entrance, the atrial sphincter itself is clearly located just proximally of the three-way junction of the membranous sac, tentacle sheath and the vestibular wall. A similar orientation was depicted by Boardman and McKinney (1985; Figure 4a) for an unidentified Alaskan species with *Disporella*-like morphology, but not in other bryozoans in their study.

A contrasting account is given in a number of tubuliporid species described by Schäfer (1985), as well as in *Crisia eburnea* (Nielsen & Pedersen, 1979), where the atrial sphincter is located more distally relative to the splitting point of the tentacle sheath and membranous sac. Nielsen and Pedersen (1979), in particular, describe a collar-like structure, an upward extension of the tentacle sheath, in which epidermal cells are situated on one side of the basement membrane and atrial sphincter muscles on the other. This 'collar' extends distally above the splitting point of the membranous sac, and transitions into the vestibular wall. The authors interpret it as a continuation of the tentacle sheath because the epidermal cells lack cuticle, which starts later, on the vestibular wall. No such extension was seen in hornerids, where the vestibular wall begins directly.

The morphology and arrangement of atrial polypide attachments and ligaments is even more variable in Cyclostomatida. Examples include a set of small spot-like attachments (Borg, 1926b; Nielsen, 1970; Schäfer, 1985; Shunatova & Tamberg, 2019), a combination of large and small attachments (Nielsen & Pedersen, 1979), and a single, almost circular structure (perimetric attachment organ of Boardman, 1973; Schäfer, 1985; and Schwaha et al., 2018). In addition, distal attachment organs may be missing altogether (Boardman & McKinney, 1985). Studies on *Crisia eburnea* by Nielsen (1970) and Nielsen and Pedersen (1979) provide different counts of polypide attachments in the atrial region: eight in the ancestrula and four in fully formed polypides.

The position of the attachment organs determines the position of the polypide within the zooidal chamber (Boardman, 1998; Boardman et al., 1992). For instance, in *Cinctipora elegans* the attachment organ sits ~700 µm from the aperture (Schwaha et al., 2018). This places a limit on how far the polypide can protrude during feeding, and the depth to ligaments is positively correlated with the length of the tentacle sheath (Boardman et al., 1992). Indeed, the full tentacle length for this species is ~600 µm, but in feeding animals more than a quarter of this length may be hidden below the aperture rim (Tamberg & Smith, 2020).

Boardman (1998) examined several hornerid species from the Arctic, Antarctic, Mediterranean and New Zealand. He reported

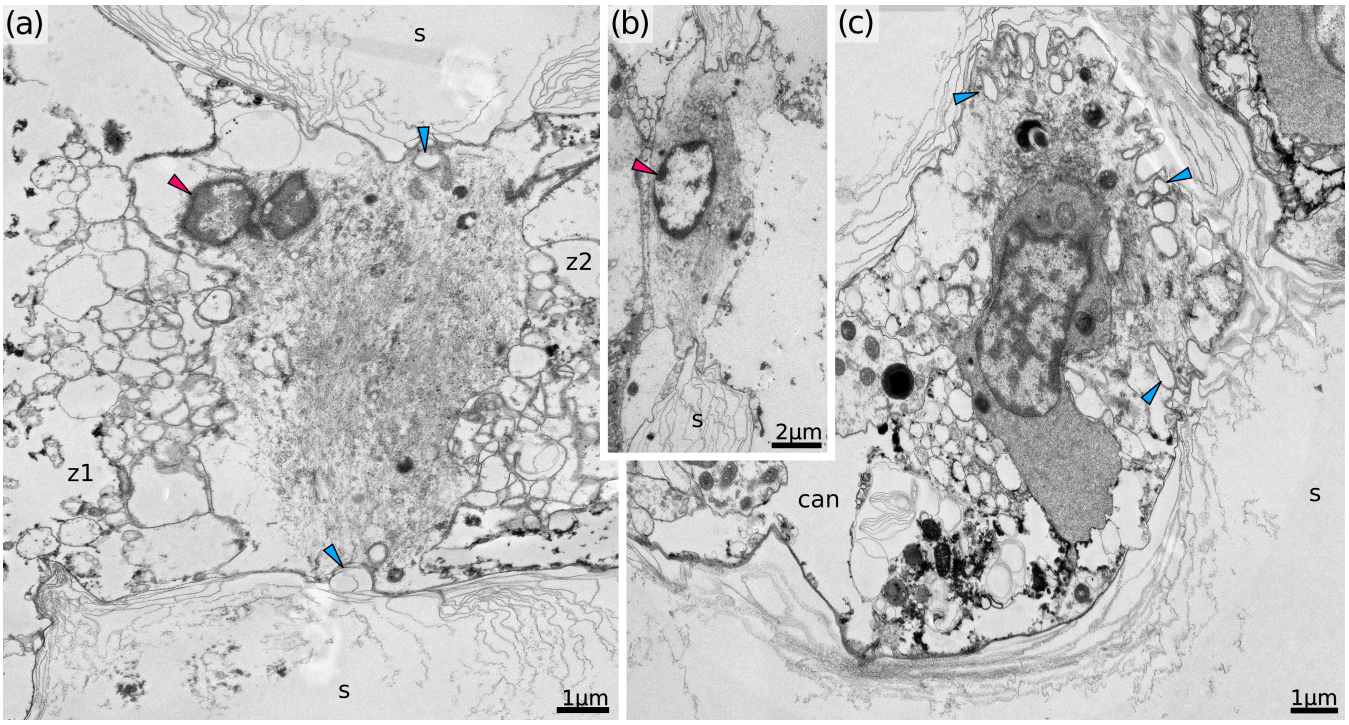

FIGURE 15 Interzooidal and hypostegal pores of *Hornera robusta*. (a,b) Transverse section of the interzooidal pores. Note the absence of endocyst cells in contact with pore cell in one of the zooids on (b). (c) Obliquely longitudinal section of the mural pore between a zooid and cancellus. *can, cancellus; s, skeleton; z1, z2, autozooids on either side of the pore; blue arrowhead, skeletal spines in the central plane of the pore; red arrowhead, nucleus of the pore cell*

dissimilar distal attachments in different species, ranging from weak and membranous, to thick and well-developed. Our results are also variable: in Horneridae gen. sp. 3 the attachment organ is large, with multiple ligaments, while in the three examined *Hornera* species it is completely missing. Such a disparity prompted us to pay extra attention and double-check this observation. Based on a number of complete serial sections (including a gap-free SBF-SEM dataset from Tamberg et al., 2021), we are assured that the distal attachment organ is absent in *H. robusta*, at least some of the time. Interestingly, the absence of atrial attachments goes against the general trend reported by Boardman (1998) for cyclostomes with progressive polypide cycles. However, he also reported a 'fragile' attachment in an unidentified species of *Hornera* from Otago shelf of New Zealand, which he considered to be pulled off the wall (figure 32), but which may have been missing altogether.

The taxonomy of the group is notoriously difficult to unravel (Smith et al., 2008), especially given the unusually high hornerid diversity in New Zealand waters. In view of recent research, it is probable that what Boardman (1998) considered three New Zealand species of *Hornera* came from two or more different genera. The magnitude of dissimilarities in his study agrees with those reported here between *Hornera* spp. and Horneridae gen. sp. 3. As previously suggested by Schäfer (1985) and Boardman and McKinney (1985), the presence and organisation of the atrial attachments may be a useful taxonomic character. Our findings point towards the genus level as most informative for Horneridae, but this may vary for other families.

Vestibular dilators (ectodermal longitudinal muscles) connect the atrial region of the zooid with the terminal membrane and play a role in opening the orifice and in redistribution of body fluid during polypide protrusion. These muscles were originally described by Borg (1926-b) and were later found in *Crisia* (Nielsen & Pedersen, 1979; Worsaae et al., 2018), but not in *Cinctipora* (Schwaha et al., 2018). Worsaae et al. (2018) related their presence to the fixed vs. free-walled condition of these respective species. We can provisionally confirm vestibular dilators in hornerids, although we were unable to locate insertion points of the muscles on the terminal membrane. A confocal laser scanning microscopic examination with phalloidin staining can best examine this question.

Nielsen and Pedersen (1979) described the vestibular walls as being made of a single, uninterrupted layer of ectodermal cells, covered with cuticle, but lacking ECM. The same traits are present in *Hornera*, but there is also a major difference: distinct epithelium is only present in the proximal quarter of the vestibular wall, with loose cell aggregations or naked cuticle extending distally above this point. A similar situation is present in *C. elegans* (Figure 6 in Schwaha et al., 2018).

Epidermal cells in the proximal part of the vestibulum have a unique appearance compared to the rest of the epidermis. They are engaged in active biosynthesis, as evidenced by enlarged rER and extensive Golgi fields. We propose that their primary role lies in production (or renewal) of the body wall cuticle, especially given the lack of indications of biosynthesis in the cells underlying the cuticle elsewhere in the zooid or the colony. At the light-microscopic level,

proximal vestibulum is easy to mistake for the atrial sphincter itself, as did Boardman (1998; see his figure 31).

The organisation of the orifice seems to differ considerably among cyclostomes. Nielsen and Pedersen (1979) described a presumed orificial sphincter made of non-muscular cells, which are nonetheless rich with contractile microfilaments. Boardman and McKinney (1985) reported orificial muscles in *Pustulipora* sp. and in a *Tubulipora* species, although there are no photographs and no further information on their composition and ultrastructure. However, a majority of species in their study are depicted without a distal closure at the top of the vestibulum. The same applies to *Cinctipora elegans* (Schwaha et al., 2018). In these taxa the terminal membrane cannot be distinguished from the vestibular wall, the vestibular space takes the form of a funnel, and the orifice coincides with the atrial sphincter. In Horneridae gen. sp. 3 we noticed a similar situation in some zooids, whereas in the three *Hornera* species examined here the terminal membrane stretches more or less transversely across the aperture and the vestibulum exists as a narrow cylindrical space. Even without specialised muscles, the orifice in this genus is separate from the atrial sphincter. Its closure could potentially be effected by redistribution of exosaccal cavity fluid alone given enough cuticle area.

The terminal membrane has rarely been studied directly. Nielsen and Pedersen (1979) describe a layer of large, irregularly-shaped cells underlying the terminal membrane cuticle, and indicate the insertion points of the vestibular dilators. Later studies on *Crisia* confirm that the distal, branching ends of these muscles attach to the terminal membrane but give no further details about its structure (Worsaae et al., 2018). In hornerids, we rarely observed a complete cell layer under the terminal membrane.

4.2 | Characteristics of bryozoan epithelia

Cell continuity, implemented by cell junctions, the presence of extracellular supporting matrix and aligned apical-basal cell polarisation are the three defining traits of any epithelium (Rieger, 1986; Schmidt-Rhaesa, 2007; Tyler, 2003). All bryozoans examined to date, including the hornerid species studied here, possess all three signature traits: cell contacts in the form of belt desmosomes and septate junctions, ECM layers, varying from fine to robust, and finally, apical structures (cilia, microvilli, cuticle) and secretory granules unambiguously representing cell polarisation (e.g., Mukai et al., 1997). Yet, in this study we found unusual epithelial characteristics in the epidermis of the cystid, the terminal membrane and the vestibular wall (but not tentacle sheath). The examined hornerids, and also some other bryozoans, demonstrate four striking departures from the standard epithelium model.

4.2.1 | Endocyst with missing ECM

Portions of the body wall, locally missing ECM (and periotoneum) are reported in all bryozoan groups except Phylactolaemata (Mukai et al., 1997). Invariably, this body wall condition occurs in conjunction with the presence of ectocyst, regardless of its composition. Cyclostomates in which portions of the epidermis are missing ECM were described by Nielsen and Pedersen (1979) and Shunatova and Tamberg (2019). This situation is also known in gymnolaemates: cheilostomes (Banta, 1971; Mukai et al., 1997; Shunatova & Tamberg, 2019) and, presumably, ctenostomes (Schwaha & De Blauwe, 2020). On the surface these cases appear incompatible: in Gymnolaemata the body wall underlying the skeleton is missing ECM and coelotheliumin. In Stenolaemata, however, both are preserved in a detached form as the membranous sac. Yet the remaining endocyst epidermis, which should be capable of secreting ECM on its own, does not do so in both cases.

Nielsen and Pedersen (1979) called the exosaccal cavity of cyclostomes 'pseudocoelic' (as opposed to 'coelomic'). A recent model describing pseudocoel, or primary body cavity formation calls this position into question. According to Schmidt-Rhaesa (2007); also see Ruppert, 1991), the primary body cavity originated as a series of slits forming within the ECM matrix of the organism and enlarging with increase in body fluid volume/pressure. Thus, the entire cavity has to be lined by 'naked' ECM to be rightly called pseudocoel. In cyclostomes, only one of the walls has ECM. Other walls (endocyst and vestibular wall for exosaccal cavity; inner and outer layers of the outer colonial wall for hypostegal cavity) are made of epidermal cells unsupported by ECM. One may speculate that the latter has been lost, but further studies, especially of zooid formation and polypide regeneration, are needed for better understanding.

4.2.2 | Shared colonial wall without ECM

Borg (1926a, 1926b) described the outer free colonial wall as having a thin but distinctive cellular lining ('mesoderm') under the epidermis, and considered exosaccal and hypostegal cavities to be coelomic. Later works repeated this view, re-designating 'mesoderm' as 'peritoneum' (e.g., Ryland, 1970). Nielsen and Pedersen (1979), after examination of the exosaccal cavity in *Crisia*, predicted that the hypostegal cavity in free-walled cyclostomes should be non-coelomic and have the same organisation as the exosaccal cavity. This prediction, although compelling, has never been checked before. Our results confirm Nielsen and Pedersen's expectation, at least in hornerids. Inasmuch as the hypostegal cavity is the extension of exosaccal cavity beyond the limit of an individual zooid, the cell linings of the colony wall are the extensions of the endocyst and the composition of these walls is similar.

At the same time, the original observations by Borg (1926a, 1926b) cannot be dismissed, and indeed were partly confirmed here and also by Nekliudova et al. (2021) in substance if not in interpretation. Although numerous TEM images confirm the lack of collagenous ECM supporting much of the epidermis, we saw squamous, seemingly epidermal, cells making up a loose 'secondary layer' in various parts of the colony.

It is not clear why epidermis along both outer and inner linings of colony walls (i.e., the respective cuticle- and skeleton-secreting membranes) is missing protein components of ECM (the presence of polysaccharide materials cannot be dismissed, but is not relevant as an epithelium-defining character). Presumably, the cells secreting skeletal wall do not need additional structural support from ECM, perhaps because they are in direct contact with other robust supporting elements. Cells on the outer wall layer, however, have no other structural support or barrier except for a remarkably thin exterior cuticle, despite the fact that basal secretion of the ECM and apical secretion of the cuticle are not mutually exclusive (Schmidt-Rhaesa, 2007).

4.2.3 | Epidermis without cell continuity

Except for the neighbouring tendon cells forming the attachment zones, no definite cell contacts were detected in the epithelia lining zooidal chambers (cf. visible cell junctions in the endocyst of *C. eburnea*, Figure 3 in Nielsen & Pedersen, 1979) or in the outer colonial body wall of hornerids. In mature hornerid polypides, adjacent endocystal cells do not always touch each other or pore cells, so the corresponding cell junctions are also missing. The role of cell–cell contacts lies primarily in cell adherence and/or sealing a compartment against leakage. Thus, discontinuous epithelia are relatively easy to explain inside the zooid chambers adjoining skeletal walls, but puzzling in the outer colonial body wall.

Calcification of the inner surfaces of zooid chambers is completed relatively early in zooid life (as evidenced by similar thickness of interzooidal walls at the tip and near the base of the colony), and the demand for persistent skeletal repair inside them is likely low. Thus, there is presumably little need to maintain a dense, metabolically active epithelium across most of zooid inner surface, and a similarly low need for mechanical cohesion when cells can rest directly on the skeletal wall. An existing cytological model of the growth tip extension in cyclostomes, proposed by Tavener-Smith and Williams (1972) for cheilostomes and for *Crisidia cornuta* appears to support this view, although our preliminary observations on hornerid growing tips contradict their model (a palisade cell cap does not appear to be present in *Hornera*).

The outer colonial wall, by contrast, undergoes a continuous twofold remodelling, which includes secondary calcification and cuticle expansion and maintenance (as well as possible responses to injury and predation damage). Inner (skeleton-secreting) and possibly outer (cuticle-secreting) hypostegal epithelia are engaged in these processes throughout the life of the hornerid colony. We would expect to see the need for both mechanical support and sealing of the internal environment against material loss there, but neither is reflected in epidermis structure of the imaged hornerid species.

Interestingly, the attachment zones of the membranous sac to the zooid walls are the only remnants of the baseline coelomate body wall configuration, namely: epidermis in the form of tendon cells to ECM to coelothelium of the membranous sac (Figure 16), and, as previously noted, the only cell junctions were also found between tendon cells (Figure 12f). Note the position of the junctions: they occur in the apical parts of the cells (next to the skeleton), which indicates that—at least in this part of the epidermis—the original cell polarity is preserved (see Tyler, 2003). One may argue that cell junctions between tendon cells are retained because of the need for coherence of the ligament in the face of high tensile stresses, although the septate junctions we observed appeared relatively weak (for detailed interpretation consult Jonusaite et al., 2016).

Another, but very different, example of non-continuous cell cover is found in phylactolaemates—specifically, in their podocyte-like coelothelial cells in the forked canal, the epistome and the bases of the anal tentacles. In this case, the cell cover has a normal density, but the lateral sides are interdigitated and there are narrow gaps between them, revealing the ECM beneath. This configuration is suggestive of an ultrafiltration role (Gruhl et al., 2009; Tamberg & Shunatova, 2017).

Apart from these two dissimilar cases, no other reports of bryozoans lacking cell-to-cell junctions are known: cheilostomes and phylactolaemates examined so far retain cell junctions in the epidermis (cheilostomes—Shunatova & Tamberg, 2019, Figure 13b,

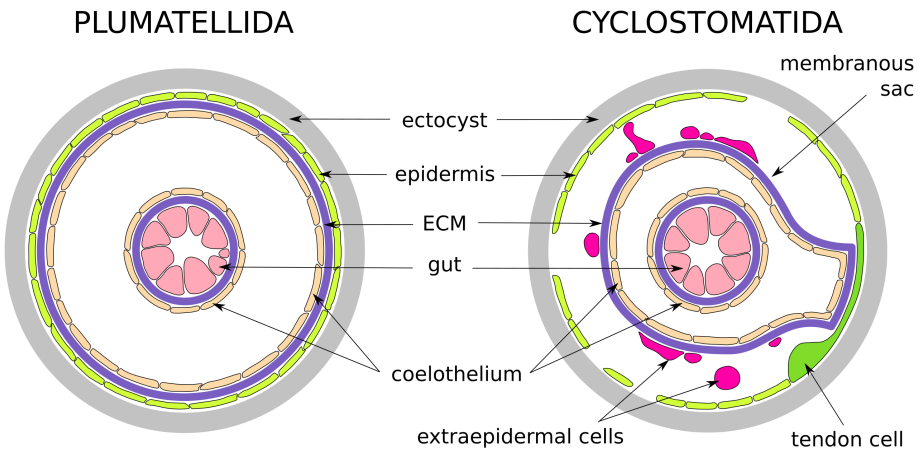

FIGURE 16 Schematic drawings of the coelomate body wall organisation in Phylactolaemata (typical) and Cyclostomatida (modified)

phylactolaemates—Mukai et al., 1997, Figures 11 and 12; Shunatova & Tamberg, 2019, Figure 4e).

4.2.4 | Two-layered coelothelium

Some studies report a curious departure from a one-cell-thick epithelium in a variety of bryozoans. The lateral sides of the tentacle coelom are lined with two coelothelial cell types, termed 'exposed' and 'enclosed' peritoneal cells, or epi- and subperitoneal cells, respectively. Subperitoneal cells are in contact with the tentacle ECM and presumably extend (as single cells) from the base all the way to the tentacle tip. The apical surface of a subperitoneal cell never comes in contact with coelomic lumen of the tentacle. Instead, this cell is completely covered by epiperitoneal cells. The latter also come in contact with ECM (on either side of subperitoneal cell) and face the tentacle coelom. Epiperitoneal cells have normal dimensions, so that numerous cells fit along the tentacle length. This arrangement has been reported in some phylactolaemates (Gruhl et al., 2009; Mukai et al., 1997; Tamberg & Shunatova, 2017); gymnolaemates and stenolaemataes (Shunatova & Tamberg, 2019).

4.2.5 | Non-epithelial cells of the body wall and exosaccal cavity

In addition, in the present study we found a number of non-epithelial cellular elements in the non-coelomic exosaccal/hypostegal cavities. The most striking example is the outer cellular covering (and potential partial epithelisation) of the membranous sac. Others include oval-shaped free cells with electron-dense cytoplasm found in the exosaccal cavity, and loose 'secondary layers' of squamous cells sometimes associated with the epidermis of the proximal vestibulum, the outer body wall and distal vestibular wall. Non-coelomic body cavity cells (variously termed amebocytes, haemocytes, etc.) are well-known in pseudocoelomates, that is, in nematodes (Bird & Bird, 1991) and priapulids (Storch, 1991). As for the cells in apparent association with various surfaces (most notably the membranous sac), one may raise the question of their potential epithelial status. Some of these cells resemble 'upper cell complex' and 'mesothelial' cells recently described by Nekliudova et al. (2021) in two crisiid species. The 'mesothelial' cells, which are presumed to work as non-coelomic mesenteria and assist in nutrient transport across crisiid colonies, deserve additional attention. In this study, similar cells were observed in the exosaccal cavity, seemingly touching both the membranous sac and the endocyst of all hornerid species. However, they were most commonly and clearly seen in retracted polypides, where the exosaccal cavity is reduced to a narrow gap between the membranous sac and the zooid wall. A high-magnification study, especially a gap-free dataset obtained with serial block-face SEM, of protruded polypides could best confirm the existence of the proposed 'mesothelial' cells in Horneridae and in other cyclostomes.

It is possible that some cell contacts are present in these cells but were not detected in this study. A more reliable detection mechanism would involve an immunolabelling study, targeting specific proteins. It is known that cell polarisation is determined by the localisation of membrane-associated proteins responsible for cell–cell contacts and anchoring to ECM (Tyler, 2003). A study detecting such proteins may determine polarity of the extraepidermal cells adhering to various surfaces inside the exosaccal cavity, as well as the cells of the endocyst and outer body wall, which are missing ECM.

4.3 | Implications for nutrient transport

The manner of nutrient transport within feeding zooids (intrazooidal), and from them to budding zones, gonozooids and other non-feeding heteromorphs (intracolonial), has attracted the attention of researchers investigating all bryozoan classes. In the absence of a specialised circulatory system, movements of the body cavity fluid and the funiculus/funicular network have been proposed to perform transport. One potential mechanism is common to all members of the phylum—fluid mixing in the body cavity induced by protrusion and retraction of the polypide. Otherwise, different bryozoan groups employ these systems differently.

To examine intrazooidal transport, we need first to look at the source of the nutrients. The principal source is the gut, but epidermal cells in direct contact with sea water (such as tentacle sheath lining) also uptake dissolved organic molecules: amino acids and simple sugars (see Gordon et al., 1987 and references therein; Johnson & Wendt, 2007). We assume, however, that this source alone cannot fulfil all nutritional requirements of the epidermis. It is reasonable to infer that metabolite transport has to reach every part of the zooid with living cells, likely even the tentacles.

In phylactolaemates the issue of intrazooidal transport is resolved by flow of coelomic fluid. All the body cavities are confluent and massive peritoneal ciliation facilitates the flow (e.g., Gruhl et al., 2009). Gymnolaemates have only two compartments in their soft body: lophophoral coelom and trunk cavity, which are connected by two ciliated ducts (Shunatova & Tamberg, 2019). Finally, in cyclostomes lophophoral and endosaccal coeloms are fully separated by a septum (but note that a few coelothelial cells penetrate the septum and make contact with the lophophore coelom; reported here and in Shunatova & Tamberg, 2019). Additional compartmentalisation is brought about by the membranous sac. Nutrients need to traverse different boundaries depending on their destination: a peritoneal septum on the way to the lophophore (coelothelium–ECM–coelothelium), and a membranous sac (coelothelium–ECM) on the way to zooid wall epidermis, vestibular wall and atrial sphincter.

Apparently, despite their obvious role in separating compartments, septa and the membranous sac are not insurmountable barriers to the nutrient transfer. In all cases the coelothelial cells and underlying ECM are very thin (~10 μm), presenting little hindrance to diffusion. In addition, Nielsen and Pedersen (1979) reported presumed pinocytosis in

the coelothelium of the membranous sac and Nekliudova et al. (2021) described cell projections penetrating its ECM.

Intracolonial transport presents greater challenges in terms of distance and directionality of movement. Among gymnolaemates, the Ctenostomatida have a rich set of traits facilitating intracolonial transport (Schwaha et al., 2020): circulation of coelomic fluid is assisted by peritoneal cilia and contraction of transverse muscles in the stolon, whereas pore-cell complexes regulate transport through the funiculus. Cheilostomates likely rely on their complex funicular network for these purposes. Dense peritoneal ciliation present in large zooids of Phylactolaemata can potentially assist in the mixing of coelomic fluid on the colony scale.

In cyclostomes, the set of available intracolonial-transport-facilitating methods is limited, because the funiculus is not connected to interzooidal pores, and the exosaccal/hypostegal cavity has no inward-facing ciliation (and no obvious trace of muscular structures). All cyclostomes have mural pores, which may be partially open (as in distal interzooidal pores in *Crisia*; Nielsen & Pedersen, 1979) or occluded by specialised cells (as reported here). In free-walled cyclostomes there is also a continuous hypostegal cavity that provides fluid access to all parts of the colony (see Batson et al., 2021).

The exosaccal/hypostegal cavity seems like the best pathway for intracolonial metabolite transport in hornerids, but it shows no obvious anatomical traits to support this function. The free outer body wall, especially with patches of 'naked' cuticle, seems an insufficient boundary against the leakage of small-molecular-size nutrients from the body fluid. To prevent significant loss, nutrients may be stored (i.e., immobilised) inside specialised storage cells. But if so, how is metabolite transport, storage and liberation performed and regulated? Clearly, our current understanding is insufficient to answer this question. Equally clearly, however, and despite the apparent limitations listed above, hornerid bryozoans successfully accomplish ongoing secondary calcification, colonial growth and reproduction, often in parts of the colony a long distance from the nearest feeding autozooids.

ACKNOWLEDGEMENTS

We are most grateful to Ruth Napper from Department of Anatomy, to the master and crew of *R.V Polaris II*, staff at Portobello Marine Laboratory and the Otago Microscopy and Nanoscale Imaging unit (OMNI), University of Otago, as well as Minh Huynh from Sydney University. Special thanks go to Hamish Bowman, Kim Currie, Linda Groenewegen, Allan Mitchell and Richard Easingwood. Y.T. gratefully acknowledges discussion from Nina Alexeeva (Zoological Institute of the Russian Academy of Science), as well as funding from a University of Otago Doctoral Scholarship.

CONFLICT OF INTEREST

The authors declare that they have no financial or otherwise conflicts of interest.

AUTHOR CONTRIBUTIONS

Yuta Tamberg: Conceptualization (lead); investigation (lead); resources (equal); visualization (lead); writing – original draft (lead); writing – review and editing (lead). **Peter B. Batson:** Conceptualization (supporting); investigation (supporting); resources (equal); writing – review and editing (supporting). **Abigail M. Smith:** Resources (equal); supervision (lead); writing – review and editing (supporting).

PEER REVIEW

The peer review history for this article is available at https://publons.com/publon/10.1002/jmor.21451.

DATA AVAILABILITY STATEMENT

The data that support the findings of this study are available from the corresponding author upon reasonable request.

ORCID

Yuta Tamberg https://orcid.org/0000-0002-3460-3323
Peter B. Batson https://orcid.org/0000-0002-8562-4159

REFERENCES

Banta, W. C. (1971). The body wall of cheilostome Bryozoa IV. The frontal wall of *Schizoporella unicornis* (Johnston). *Journal of Morphology*, *135*(2), 165–184.

Batson, P. B., Gordon, D. P., Taylor, P. D., Negrini, M., Tamberg, Y., & Smith, A. M. (2021). *Hornera currieae*, n. sp., a novel deepwater hornerid bryozoan with skeletally preserved metabolite-translocation dynamics (Bryozoa: Cyclostomata). *Zootaxa*, *5020*(2), 257–287.

Bird, A. F., & Bird, J. (1991). Pseudocoelom. In A. F. Bird & J. Bird (Eds.), *The structure of nematodes* (pp. 157–166). Academic Press.

Boardman, R. S. (1973). Body walls and attachment organs in some recent cyclostomes and Paleozoic trepostomes. In G. P. Larwood (Ed.), *Living and fossil Bryozoa* (pp. 231–246). Academic Press.

Boardman, R. S. (1998). *Reflections on the morphology, anatomy, evolution, and classification of the class Stenolaemata (Bryozoa). Smithsonian contributions to Paleobiology. V. 86*. Smithsonian Institution Press.

Boardman, R. S., & McKinney, F. K. (1985). Soft part characters in stenolaemate taxonomy. In C. Nielsen & G. P. Larwood (Eds.), *Bryozoa: Ordovician to Recent* (pp. 35–44). Olsen & Olsen.

Boardman, R. S., McKinney, F. K., & Taylor, P. D. (1992). *Morphology, anatomy, and systematics of the Cinctiporidae, new family (Bryozoa: Stenolaemata). Smithsonian Contributions to Paleobiology. V. 70*. Smithsonian Institution Press.

Borg, F. (1926a). Memoirs: On the body-wall in Bryozoa. *Journal of Cell Science*, *2*(280), 583–598.

Borg, F. (1926b). Studies on recent cyclostomatous Bryozoa. *Zoologiska Bidrag från Uppsala*, *10*, 181–150.

Gordon, D. P., Clark, A. G., & Harper, J. F. (1987). Bryozoa. Pp. 173-199 in Pandian, T. J., & Vernberg, F. J. (Eds.). *Animal energetics: Bivalvia through Reptilia* (Vol. 2). Academic Press. .

Gruhl, A., Wegener, I., & Bartolomaeus, T. (2009). Ultrastructure of the body cavities in Phylactolaemata (Bryozoa). *Journal of Morphology*, *270*, 306–318.

Inkscape Project. 2017. Inkscape 0.92. http://www.inkscape.org/.

Johnson, C. H., & Wendt, D. E. (2007). Availability of dissolved organic matter offsets metabolic costs of a protracted larval period for *Bugula neritina* (Bryozoa). *Marine Biology*, *151*(1), 301–311.

Jonusaite, S., Donini, A., & Kelly, S. P. (2016). Occluding junctions of invertebrate epithelia. *Journal of Comparative Physiology B*, *186*(1), 17–43.

Kremer, J. R., Mastronarde, D. N., & McIntosh, J. R. (1996). Computer visualization of three-dimensional image data using IMOD. *Journal of Structural Biology*, *116*, 71–76.

Mukai, H., Terakado, K., & Reed, C. G. (1997). Bryozoa. In F. W. Harrison & R. M. Woollacott (Eds.), *Microscopic anatomy of invertebrates* (Vol. 13, pp. 45–206). Wiley-Liss.

Nekliudova, U. A., Schwaha, T. F., Kotenko, O. N., Gruber, D., Cyran, N., & Ostrovsky, A. N. (2021). Three in one: Evolution of viviparity, coenocytic placenta and polyembryony in cyclostome bryozoans. *BMC Ecology and Evolution*, *21*(1), 1–34.

Nielsen, C. (1970). On metamorphosis and ancestrula formation in cyclostomatous bryozoans. *Ophelia*, *7*(2), 217–256.

Nielsen, C., & Pedersen, K. J. (1979). Cystid structure and protrusion of the polypide in *Crisia* (Bryozoa, Cyclostomata). *Acta Zoologica*, *60*(2), 65–88.

Rieger, R. M. (1986). Über dem Ursprung der Bilateria: die Bedeutung der Ultrastrukturforschung für ein neues Verstehen der Metazoenevolution. *Verhandlungen der Deutschen Gesellschaft fur Pathologie*, *79*, 31–50.

Ruppert, E. E. (1991). Introduction to aschelminth phyla. A consideration of mesoderm body cavities and cuticle. In F. W. Harrison & E. E. Ruppert (Eds.), *Microscopic anatomy of invertebrates* (Vol. 4, pp. 1–17). Wiley-Liss.

Ryland, J. S. (1970). *Bryozoans*. Hutchinson University Library.

Schäfer, P. (1985). Significance of soft part morphology in the classification of recent tubuliporoid cyclostomes. In C. Nielsen & G. P. Larwood (Eds.), *Bryozoa: Ordovician to Recent* (pp. 273–284). Olsen & Olsen.

Schmidt-Rhaesa, A. (2007). *The evolution of organ systems*. Oxford University Press.

Schwaha, T., & De Blauwe, H. (2020). Morphology of ctenostome bryozoans: 1. *Arachnidium fibrosum*. *Journal of Morphology*, *281*(12), 1598–1606.

Schwaha, T. F., Handschuh, S., Ostrovsky, A. N., & Wanninger, A. (2018). Morphology of the bryozoan *Cinctipora elegans* (Cyclostomata, Cinctiporidae) with first data on its sexual reproduction and the cyclostome neuro-muscular system. *BMC Evolutionary Biology*, *18*(1), 92.

Schwaha, T. F., Ostrovsky, A. N., & Wanninger, A. (2020). Key novelties in the evolution of the aquatic colonial phylum Bryozoa: Evidence from soft body morphology. *Biological Reviews*, *95*(3), 696–729.

Shunatova, N., Denisova, S., & Shchenkov, S. (2021). Ultrastructure of rhizoids in the marine bryozoan *Dendrobeania fruticosa* (Gymnolaemata: Cheilostomata). *Journal of Morphology*, *282*(6), 847–862.

Shunatova, N., & Tamberg, Y. (2019). Body cavities in bryozoans: Functional and phylogenetic implications. *Journal of Morphology*, *280*(9), 1332–1358.

Smith, A. M., Taylor, P. D., & Spencer, H. G. (2008). Resolution of taxonomic issues in the Horneridae (Bryozoa: Cyclostomata). In P. N. Wyse Jackson & M. E. Spencer Jones (Eds.), *Annals of Bryozoology 2* (pp. 359–412). Aspects of the History of Research on Bryozoans. Dublin.

Storch, V. (1991). Priapulida. In F. W. Harrison & E. E. Ruppert (Eds.), *Microscopic anatomy of invertebrates* (Vol. 4, pp. 333–350). Wiley-Liss.

Tamberg, Y., Batson, P. B., & Napper, R. (2021). Polypide anatomy of hornerid bryozoans (Stenolaemata: Cyclostomatida). *Journal of Morphology*, *282*, 1708–1725.

Tamberg, Y., & Shunatova, N. (2017). Tentacle structure in freshwater bryozoans. *Journal of Morphology*, *278*, 718–733.

Tamberg, Y., & Smith, A. M. (2020). In search of predictive models for stenolaemate morphometry across the skeletal–polypide divide. *Paleobiology*, *46*, 218–236.

Tavener-Smith, R., & Williams, A. (1972). The secretion and structure of the skeleton of living and fossil Bryozoa. *Philosophical Transactions of the Royal Society of London. B, Biological Sciences*, *264*(859), 97–160.

Tyler, S. (2003). Epithelium—The primary building block for metazoan complexity. *Integrative and Comparative Biology*, *43*(1), 55–63.

Worsaae, K., Frykman, T., & Nielsen, C. (2018). The neuromuscular system of the cyclostome bryozoan *Crisia eburnea* (Linnaeus, 1758). *Acta Zoologica*, *101*(2), 133–146.

How to cite this article: Tamberg, Y., Batson, P. B., & Smith, A. M. (2022). The epithelial layers of the body wall in hornerid bryozoans (Stenolaemata: Cyclostomatida). *Journal of Morphology*, *283*(4), 406–427. https://doi.org/10.1002/jmor.21451